Article

Metabolically Stable Anomeric Linkages Containing GalNAc−siRNA Conjugates: An Interplay among ASGPR, Glycosidase, and RISC Pathways

Pachamuthu Kandasamy, Shohei Mori, Shigeo Matsuda, Namrata Erande, Dhrubajyoti Datta, Jennifer L. S. Willoughby, Nate Taneja, Jonathan O'Shea, Anna Bisbe, Rajar M. Manoharan, Kristina Yucius, Tuyen Nguyen, Ramesh Indrakanti, Swati Gupta, Jason A. Gilbert, Tim Racie, Amy Chan, Ju Liu, Renta Hutabarat, Jayaprakash K. Nair, Klaus Charisse, Martin A. Maier, Kallanthottathil G. Rajeev, Martin Egli, and Muthiah Manoharan*

Read Online

ACCESS | Metrics & More | Article Recommendations | Supporting Information

β-Anomeric Linkages

III, X= S VIII, X= CH₂ → III, X= S VIII, X= CH₂

V   VI

α-Anomeric Linkages

IV, X= S   VII, X= CH₂

Metabolically labile glycosidic linkage

Metabolically stable glycosidic linkages
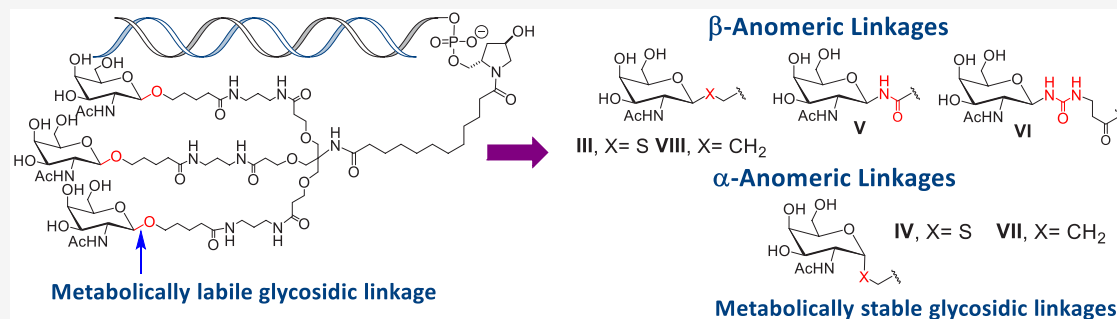
ABSTRACT: Conjugation of synthetic triantennary *N*-acetyl-ᴅ-galactosamine (GalNAc) to small interfering RNA (siRNA) mediates binding to the asialoglycoprotein receptor (ASGPR) on the surface of hepatocytes, facilitating liver-specific uptake and siRNA-mediated gene silencing. The natural β-glycosidic bond of the GalNAc ligand is rapidly cleaved by glycosidases in vivo. Novel GalNAc ligands with *S*-, and *C*-glycosides with both α- and β-anomeric linkages, *N*-glycosides with β-anomeric linkage, and the *O*-glycoside with α-anomeric linkage were synthesized and conjugated to siRNA either on-column during siRNA synthesis or through a high-throughput, post-synthetic method. Unlike natural GalNAc, modified ligands were resistant to glycosidase activity. The siRNAs conjugated to newly designed ligands had similar affinities for ASGPR and similar silencing activity in mice as the parent GalNAc−siRNA conjugate. These data suggest that other factors, such as protein−nucleic acid interactions and loading of the antisense strand into the RNA-induced silencing complex (RISC), are more critical to the duration of action than the stereochemistry and stability of the anomeric linkage between the GalNAc moiety of the ligand conjugated to the sense strand of the siRNA.

■ INTRODUCTION

Tissue-specific delivery of small interfering RNAs (siRNAs) to hepatocytes mediated by conjugation to the synthetic triantennary *N*-acetyl-ᴅ-galactosamine (GalNAc) ligand (Figure 1A), which binds to the asialoglycoprotein receptor (ASGPR) on the surface of hepatocytes, has played a major role in the development of therapies based on RNA interference (RNAi). Several GalNAc-conjugated siRNAs, including givosiran (GIVLAARI), lumasiran (OXLUMO), inclisiran (LEQVIO), and vutrisiran (AMVUTTRA), have been approved for clinical use. Givosiran is a subcutaneously administered RNAi therapeutic approved for the treatment of acute hepatic porphyria,[1] lumasiran is used for the treatment of primary hyperoxaluria type 1 in all age groups,[2] inclisiran is approved by both the EMA and US FDA for the treatment of

adults with heterozygous familial hypercholesterolemia,[3−5] and vutrisiran is used for the treatment of polyneuropathy caused by transthyretin amyloidosis in adults.[6] All of these siRNAs contain a triantennary GalNAc ligand conjugated to the 3′ end of their sense strands.

The ASGPR is a C-type lectin expressed on the surfaces of hepatocytes that binds to a broad spectrum of carbohydrate clusters bearing terminal-galactose or galactose-like residues
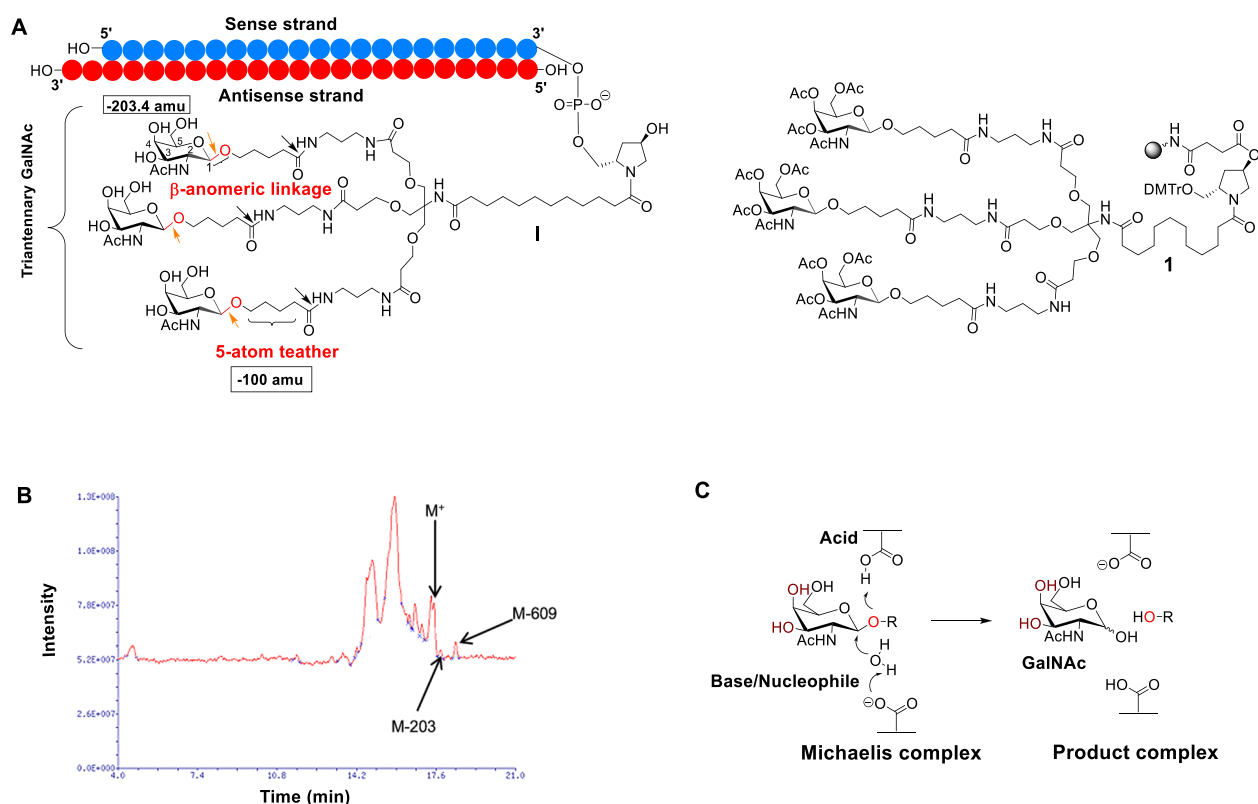
Figure 1. (A) Triantennary GalNAc–siRNA with metabolically labile β-O-glycosidic linkages. Orange and black arrows indicate predominant metabolic cleavage sites of the ligand based on mass spectral analysis of the sense strand extracted from mouse liver at 15 min post-dose. (B) Observed parent and cleavage products M, M-203 and M-609 confirm β-O-glycosidic linkages as the metabolic hot spots and are shown in the LC-MS profile. (C) Plausible mechanism of β-O-glycosidic linkage cleavage based on previous studies.
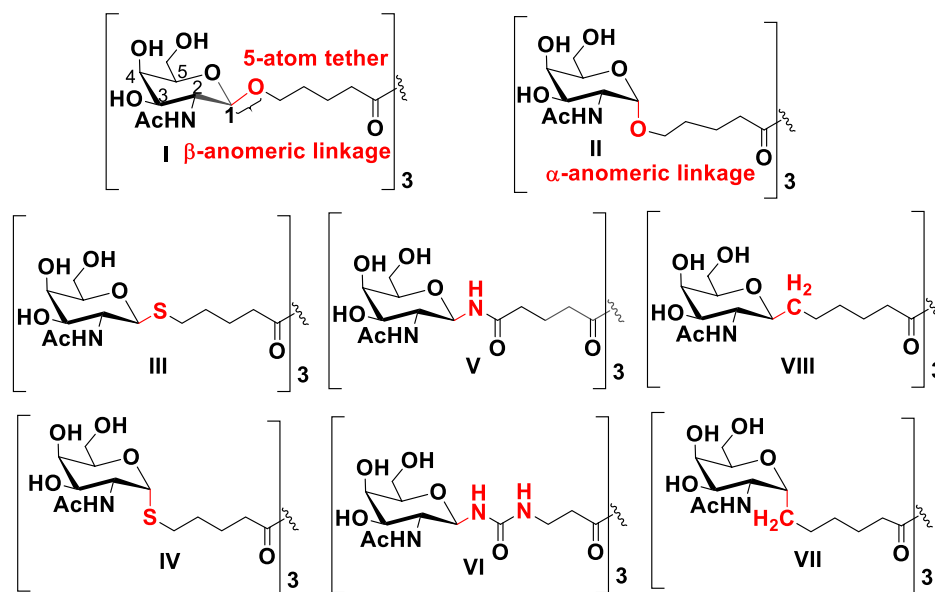
Figure 2. Triantennary GalNAc with β-O-glycosidic linkage I and chemically modified glycosidic linkages II to VIII.

such as D-fucose, D-galactose, D-lactose, and GalNAc.[7] ASGPR binds to terminal galactose residues of desialylated serum glycoproteins through Ca^{2+} chelation to facilitate the clearance of aged glycoproteins from circulation via clathrin-mediated endocytosis.[8−11] Upon acidification in early endosomes, the ligand is released and transported into the lysosomal

compartment, and the receptor is recycled back to the surface of the hepatocyte.[7]

Covalent conjugation of an engineered triantennary GalNAc to therapeutic oligonucleotides enables efficient ASGPR-mediated delivery of the oligonucleotide payloads into hepatocytes at pharmaceutically relevant doses.[1−5,12,13] Linkers with different numbers of sugar residues and different steric
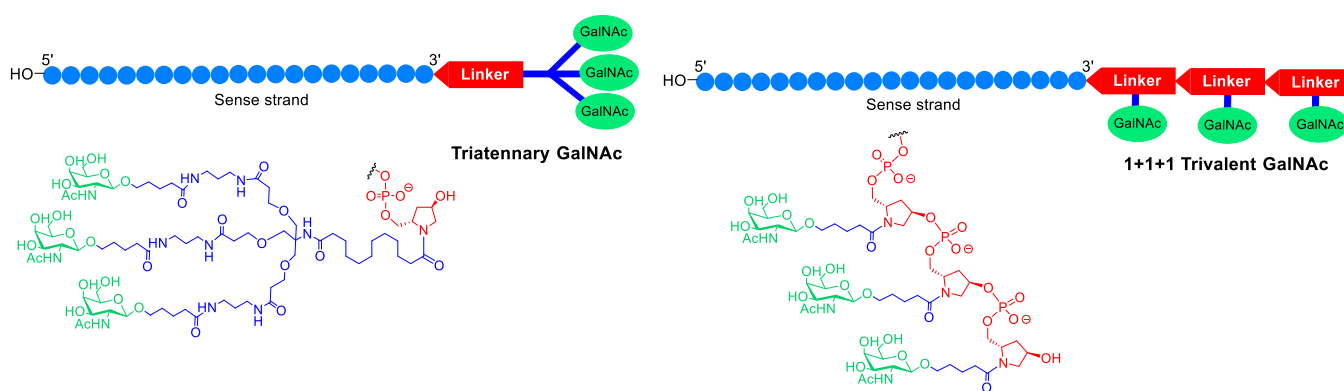
Figure 3. Cartoon of a triantennary GalNAc ligand attached to the sense strand at the 3′-end (left) and a 1 + 1 + 1 trivalent GalNAc conjugate (right).

configurations of the GalNAc clusters have been investigated.[14−17] The triantennary GalNAc ligand construct binds to the receptor with approximately 50-fold higher affinity than the ligand design terminating with galactose residues.[18,19] The stereochemistry of the hydroxyl groups at positions 3 and 4 of the GalNAc sugar moiety and its accessibility are critical for chelating with the Ca^{2+} ion to facilitate binding to the receptor.[20−22] Several glycomimetic and high-affinity ASGPR ligands have been synthesized and their binding affinities have been measured, but their therapeutic utilities have not been reported.[23−27]

In the natural ligand and in the optimized ligand mimics, the receptor-recognizing, exposed sugar moiety is covalently linked to the core assembly via the anomeric oxygen with a β-configuration (Figures 1A and S1). This natural β-O-glycosidic linkage is very susceptible to cleavage by glycosidases present in the early endosomes. Hydrolysis by a glycosidase involves general acid and general base assistance from two amino acid side chains, normally glutamic or aspartic acids, that are typically located 6−11 Å apart (Figure 1B).[28−30] The glycosidases catalyze oxygen-mediated bond cleavage, possibly also with anchimeric assistance from the C2-NHAc group. After ASGPR-clathrin-mediated endocytosis, the β-O-glycosidic bond is rapidly cleaved resulting in separation of the sugar moieties from the rest of the molecule (Figure S1). This cleavage also occurs in the context of GalNAc-conjugated siRNAs after they are taken up by hepatocytes.[31,32]

The observed short half-life of the glycosidic linkage of the triantennary GalNAc ligands in the early endosome of the hepatocytes prompted us to investigate the impact of the metabolism at the β-O-glycosidic linkage on the silencing efficacy of GalNAc-conjugated siRNAs in vivo. Metabolically stable GalNAc ligand monomers bearing S- and C-glycosides with both α- and β-anomeric linkages and N-glycosides with β-anomeric linkages were designed and synthesized (Figure 2). We generated the corresponding triantennary as well as serial 1 + 1 + 1 GalNAc ligands by post-synthetic conjugation of these sugar monomers to a triamine-functionalized sense strand containing either triantennary or serial 1 + 1 + 1 non-nucleoside GalNAc monomers.[14,15] The serial 1 + 1 + 1 format involves three GalNAc residues linked in series (Figure 3). These GalNAc−siRNA conjugates were evaluated for binding affinities to ASGPR, stability in rat tritosomes, in vitro activity under transfection and free uptake conditions in primary mouse hepatocytes, and efficacy and activity at the tissue level

(whole liver) in mice relative to the clinically validated parent β-O-glycosidic ligand.

RESULTS AND DISCUSSION

Design and Synthesis of Metabolically Stable GalNAc−siRNA Conjugates. The natural β-O glycosidic linkage was replaced at the anomeric position of the pyranose ring of the parent design **I** with GalNAc moieties containing α-O-glycosidic linkages **II**, α- and β-S-glycosidic linkages **IV** and **III**, which were previously described,[33] β-N-glycosidic linkages **V** and **VI**, which involve an amide[34] or urea,[35] or α- and β-C-glycosidic linkages **VII** and **VIII**, which were previously reported[36,37] (Figure 2). We devised a synthetic method to synthesize these ligand analogues (**17A−22A**, Scheme 1) and their activated NHS esters (**17−22**, Scheme 1) that allowed us to chemoselectively attach the GalNAc ligands to oligonucleotides containing triamine using a post-synthetic method (Scheme 2 and Table 1).

The synthesis of the GalNAc solid support **1** and the on-column synthesis of the parent GalNAc−siRNA conjugate **I** from the solid support were reported earlier from our laboratory.[12] For the post-synthetic approach, the trifluoroacetamidylated triamine solid support **2** (Scheme 3) was designed and synthesized based on a retrosynthetic analysis to obtain the fully deprotected, triamine-functionalized sense strand **3** shown in Scheme 2. Post-synthetic conjugation of NHS ester **4** to the triamine-conjugated oligonucleotide **3** yielded the triantennary GalNAc-conjugated sense strand that, upon annealing with the antisense strand afforded the conjugate **I** (Scheme 2). Use of modified sugar NHS esters **16−22**, afforded sense strands conjugates **II−VIII** (Scheme 2, Figure 2 and Table 1).

The general approach for the synthesis of NHS esters **4** and **16−22** from their corresponding carboxylic acid precursors **4A** and **16A−22A** is depicted in Scheme 1. Briefly, β-O-glycoside NHS ester **4** was synthesized as described;[12] α-O-glycoside NHS ester **16** was synthesized from the olefin **16B** through oxidative cleavage of the double bond to the carboxylic acid **16A** and subsequent NHS ester coupling.[12] The NHS esters **17** and **18** of β- and α-S-glycosides were synthesized from oxazoline **17D**[38] or thiazoline **18E**.[39]

The galactopyranosylamine **19B**[34,40−44] was converted to NHS ester **19** containing an amide linkage and **20** containing a urea linkage (Scheme 1). Finally, α- and β-C-glycosides **21** and **22** were synthesized from the corresponding allyl precursors **21B**[36] or **22E**[37] via olefin metathesis and subsequent

Scheme 1. Synthesis of Activated Esters of Modified GalNAc Carboxylic Acids[a]
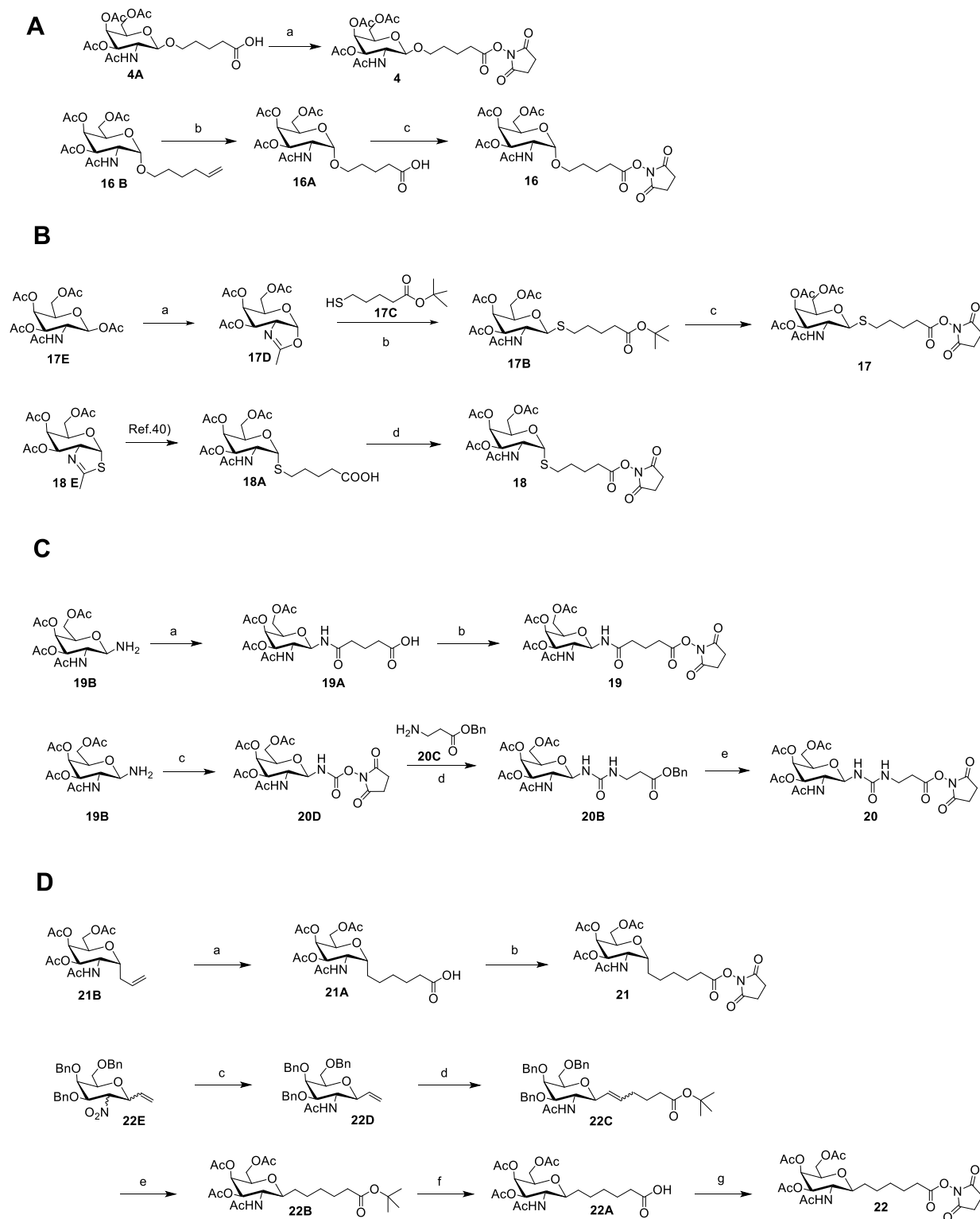
[a]Reagents and conditions: (A)—(a) NHS/EDC/CH₂Cl₂, 97%, (b) RuCl₃·H₂O/NaIO₄, 77%, and (c) NHS/EDC, 82%; (B)—(a), (b) TMSOTf/DCE, 15%, (c) (i) TFA/CH₂Cl₂ and (ii) NHS/EDC/CH₂Cl₂, 69%, and (d) NHS/EDC/CH₂Cl₂, 63%; (C)—(a) Glutaric Anhydride/Pyridine/DMAP, 86%, (b) EDC/NHS/CH₂Cl₂, 65%, (c) DSC/CH₃CN, 95%, (d) Et₃N, 80%, and (e) (i) H₂/Pd–C, (ii) NHS/EDC/CH₂Cl₂, 35%; (D)—(a) (i) Second Generation Grubb's Catalyst/Benzyl 4-Pentenoate, (ii) H₂/Pd–C/EtOAc, 39%, (b) EDC/NHS/CH₂Cl₂, 76%, (c) (i) LAH/THF, (ii) Ac₂O/DMAP/Pyridine, 25%, (d) 5-Hexenoic Acid *tert*-Butyl Ester/Second Generation Grubb's Catalyst/CH₂Cl₂, 68%, (e) (i) H₂/Pd–C/EtOAc, (ii) Ac₂O/DMAP/Pyridine, 95%, (f) TFA/CH₂Cl₂, and (g) NHS/EDC/CH₂Cl₂, 63%, Two Steps

hydrogenation. Each carboxylic acid obtained was stirred with NHS in the presence of EDC and DIEA at ambient temperature for 12−14 h to obtain the corresponding NHS ester with a moderate to high yield.

Scheme 2. On-Column Synthesis of Sense Strand 3 and Post-synthetic Conjugation of GalNAc and Anomeric Linkage-Modified GalNAc to siRNA[a]
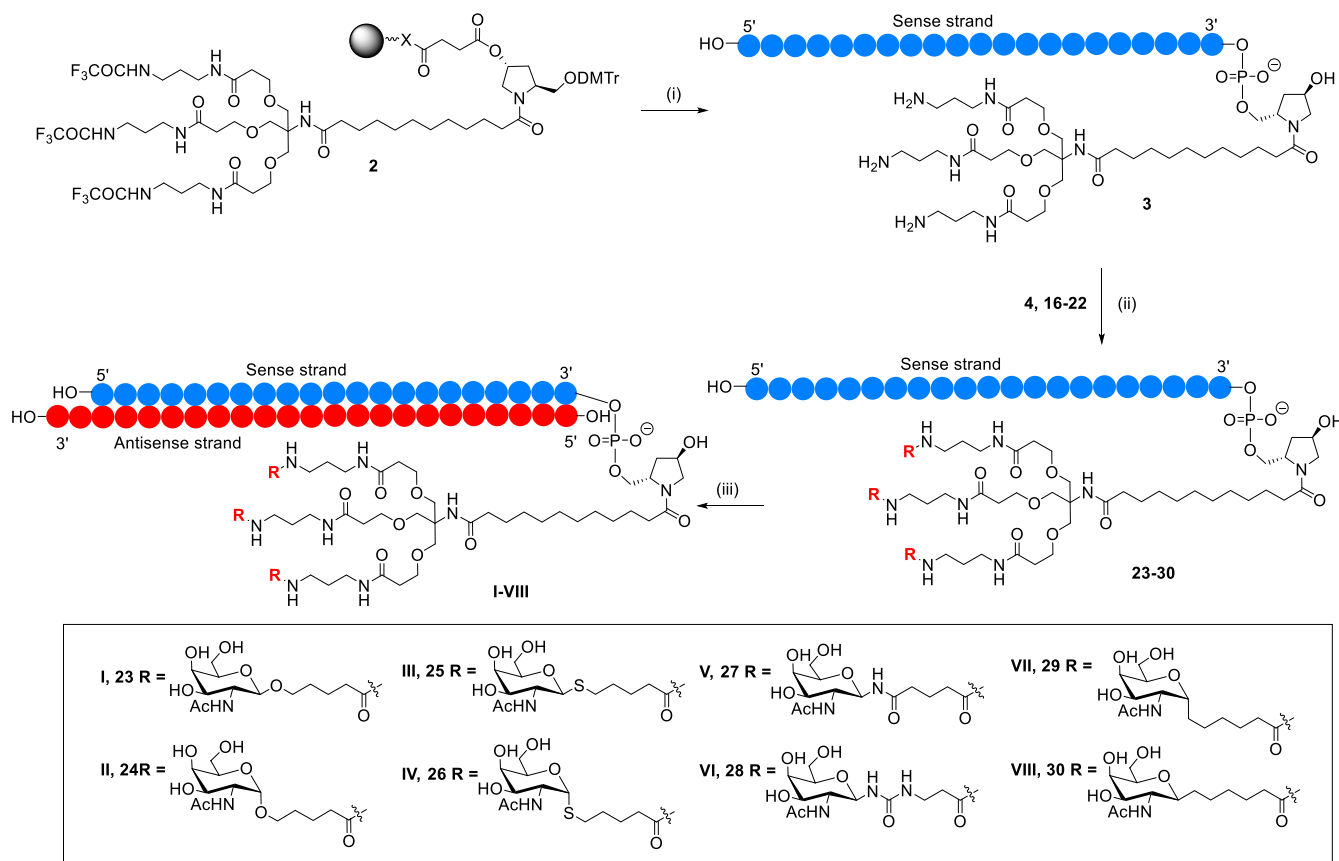
[a]The nucleotides of the sense strand are indicated by blue beads and those of the antisense strand by red beads. (i) On-column synthesis and deprotection; (ii) buffer, pH 7.2, room temperature, 4 h; and carbohydrate deprotection (iii) annealing with a complementary antisense strand.

Post-synthetic conjugation of GalNAc and anomeric linkage-modified GalNAc NHS esters **4** and **16−22** to the triamine-functionalized sense strand **3** afforded the corresponding triantennary sugar-containing sense strands **23−30** (Scheme 2). The sense strand was synthesized from the solid support **2** under standard solid-phase oligonucleotide synthesis and deprotection conditions.

The sense strand **3** was chemoselectively coupled with the desired NHS ester in a buffer at pH 7.2 to obtain the corresponding triantennary GalNAc-conjugated sense strand. Deprotection of the acetate on the sugar moieties under an aqueous methylamine condition at room temperature for 4 h gave completely deprotected GalNAc-conjugated sense strands **23−30** in good yields after HPLC purification. The integrity of each modified sense strand was confirmed by LC−MS analysis (Table S1). Annealing of the sense strands with equimolar amounts of the antisense strands afforded the siRNAs **I−VIII** (Figures 1 and 2, Table 1).

We demonstrated previously that serial presentation of three GalNAc moieties in a GalNAc−siRNA conjugate can elicit robust gene silencing similar to the parent triantennary conjugate design upon subcutaneous administration in mice, so long as the proximity of the sugar moieties and the flexibility of the tether connecting individual sugar moieties to the central core are maintained.[14] In the present study, in addition to the parent design **I**, we evaluated one of the most active alternate triantennary ligands, the 1 + 1 + 1 design **IX**, that we

described previously.[14,15] This design was functionalized with anomeric linkage-modified sugar moieties to obtain conjugates **X−XVI** (Table 1).

In Vitro Binding Affinities to ASGPR and Target Gene Silencing by Novel GalNAc−siRNA Conjugates. The binding affinities of the GalNAc−siRNA conjugates to ASGPR were determined using a fluorescence-based assay in freshly isolated primary mouse hepatocytes.[12] The inhibitory constants (K_i values) for each GalNAc-conjugated siRNA are shown in the Table 1. The binding affinities of the siRNAs conjugated to the α anomers of C- and S-linked GalNAc (siRNAs **VII** and **IV**, respectively) were enhanced by two-fold compared to siRNA **I**, which is conjugated to the parent β-O-glycoside. In contrast, the affinities of α-O- (siRNA **II**) and β-N-, (siRNAs **V and VI**) C-, and S-glycosides (siRNAs **VIII** and **III,** respectively) had 2−3 fold decreases in binding affinity. The siRNAs conjugated to 1 + 1 + 1 ligand designs (siRNAs **IX−XVI**) generally exhibited lower affinity for ASGPR than the triantennary conjugates (siRNAs **I−VIII**). This may be a result of the shorter tether lengths employed in the case of 1 + 1 + 1 designs.

We previously demonstrated that siRNAs **I** and **IX**, bearing the triantennary and 1 + 1 + 1 GalNAc ligands,[14,15] elicit robust in vitro gene silencing in primary hepatocytes under free uptake and transfection conditions. The in vitro potencies, as measured by half maximal inhibitory concentrations (IC_{50}) determined from dose−response curves in primary mouse

Table 1. Receptor Binding Affinity and IC$_{50}$ Values for Gene Silencing of Triantennary GalNAc-Conjugated siRNAs I−VIII and IX−XVI

GalNAc-conjugated siRNA[a] R =	Receptor binding K_i (nM)[b]	IC$_{50}$ (nM)		siRNA sense strand
		Transfection	Free uptake	
I	10.1 ± 2.3	0.023	1.34	5′-*A•a•CaGuGuUcUuGcUcUaUaA*X-3′ (siRNAs **I-VIII**)
II	19.4 ± 3.4	0.022	0.96	
III	34.6 + 7.2	0.024	1.24	
IV	4.8 ± 1.0	0.019	0.64	
V	18.5 ± 3.0	0.029	0.99	
VI	20.5 ± 3.7	0.041	0.97	
VII	4.2 + 0.7	0.021	0.47	
VIII	63.8± 8.3	0.022	0.28	
IX	32.0 ± 3.9	0.032	1.79	5′-*AaCaGuGuUcUuGcUcUaUaA*X-3′ (siRNAs **IX-XV**)
X	29.1 ± 4.0	0.019	0.77	
XI	53.6 ± 15.1	0.039	1.73	
XII	8.6 ± 1.0	0.043	0.59	
XIII	93.2 ± 31.0	0.021	1.04	
XIV	70.5 ± 8.4	0.022	0.83	
XV	8.8 ± 0.4	0.020	0.36	
XVI	265± 67.8	0.041	0.92	5′-*A•a•CaGuGuUcUuGcUcUaUaA*X-3′ (siRNA **XVI**)

^{a}[a] The siRNAs target mouse *Ttr*. The different sense strands used are shown in the last column of the Table and the antisense strand is common to all these sense strands is 5′-u•*U*•aUaGaGcAaGaAcAcUgUu•*U*•u-3′, where uppercase italics and lower-case letters indicate 2′-deoxy-2′-fluoro and 2′-*O*-methyl sugar modifications, respectively, to adenosine (A), cytidine (C), guanosine (G) and uridine (U); • indicates phosphorothioate linkage; and X shown in red indicates the GalNAc ligand. ^{b}The deviation indicates standard error.

hepatocytes, with and without transfection reagent, for conjugates II−VIII and X−XVI and parent siRNAs I and IX are listed in Table 1. To allow comparisons of intrinsic potencies, the cells were incubated with GalNAc−siRNA conjugate in the presence of lipofectamine RNAiMAX transfection agent. Under these conditions, in which binding affinities for the ASGPR are not expected to impact potency,

IC$_{50}$ values were found to be comparable within experimental error. Under free uptake conditions, the IC$_{50}$ values for the siRNAs with different sugar anomeric modifications varied over a five-fold range, reflecting interactions of the ligand-conjugated siRNA with ASGPR.

Modeling of the GalNAc Interaction with ASGPR. To study how metabolically stable GalNAc ligand monomers

Scheme 3. Synthesis of Solid Support 2[a]
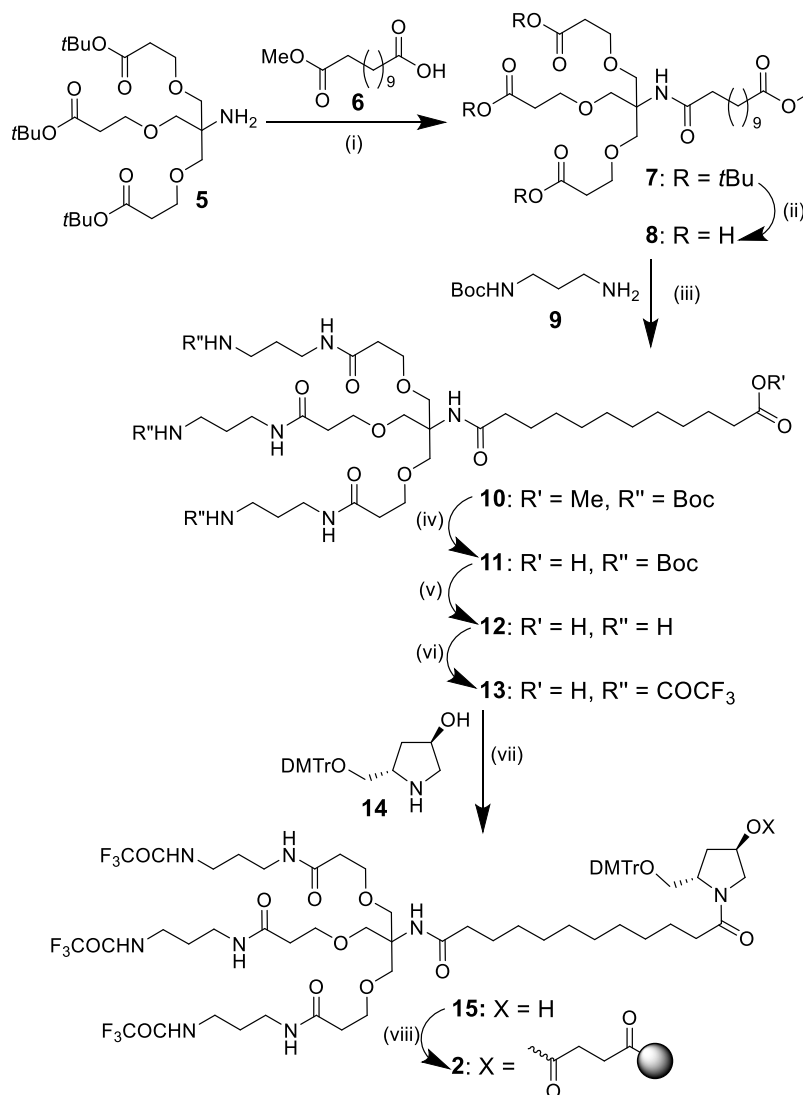
[a]Reagents and conditions: (i) EDC·HCl/HOBt, Room Temperature, 97%; (ii) HCOOH, 48 h; (iii) EDC·HCl/HOBt, Room Temperature; (iv) LiOH/THF:H₂O (3:1), Room Temperature, 14 h; (v) 4 M HCl in Dioxane; (vi) CF₃COOEt/Et₃N, 48 h; (vii) HBTU/HOBt/DCM/DMF; and (viii)—(a) Succinic Anhydride/DMAP/DCM; (b) HBTU/DIEA/lcaaCPG; and (c) Ac₂O/Py, Room Temperature, Loading: 58 μmol/g

interact with ASGPR, we modeled GalNAc with either an α-O-glycosidic linkage (I) or a β-O-glycosidic linkage (II) bound to ASGPR based on the available crystal structures of the ASGPR carbohydrate recognition domain (CRD; Figure 4A,B) and complexes between ASGPR-CRD and carbohydrates.[14,15] Both α and β configurations are compatible with binding, and steric repulsions can be avoided (Figure 4C). The stereochemistries at positions 2, 3, and 4 of the pyranose sugar moiety, which are critical for Ca²⁺-mediated binding to the receptor,[20] and the 5-atom tether length between the anomeric oxygen and amide linkage of the parent design were maintained in all ligand derivatives evaluated. Altering the stereochemistry at position 4 from axial to equatorial disrupts Ca²⁺-chelation and hence binding to the receptor,[12] and modeling further confirmed the incompatibility (Figure 4D). Modeling also suggested that substitution of the anomeric oxygen with sulfur, nitrogen, or carbon or a change of the anomeric linkage configuration from β to α would have little or no impact on binding to ASGPR (Figure 4C).

Efficacy and Duration of GalNAc−siRNA Conjugates In Vivo. We next evaluated the efficacy in mice of all the sugar-modified conjugates bearing the triantennary GalNAc ligand designs at three doses (0.3, 1, and 3 mg/kg) given subcutaneously. As a measure of gene silencing, circulating TTR protein levels were monitored; these levels correlated with mRNA depletion, as previously reported.[11,12] As expected based on previous analyses,[11,12] the siRNA conjugated to the parent β-O-GalNAc (siRNA I) elicited robust gene silencing with a median effective dose (ED₅₀) of 1 mg/kg. The siRNAs II−VII reduced circulating TTR protein by approximately 20, 60, and 80% after single, subcutaneous doses of 0.3, 1, or 3 mg/kg, respectively, similar to reductions induced by the parent siRNA I (Figure 5).

Next, the durations of action of these conjugates were studied. Upon subcutaneous administration of a single 3 mg/kg dose of siRNAs I−VII, levels of circulating TTR protein were reduced by at least 80% at 4 days post-dose relative to animals treated with the PBS control (Figure 6). Maximum TTR protein reduction of at least 90% was observed 13 days
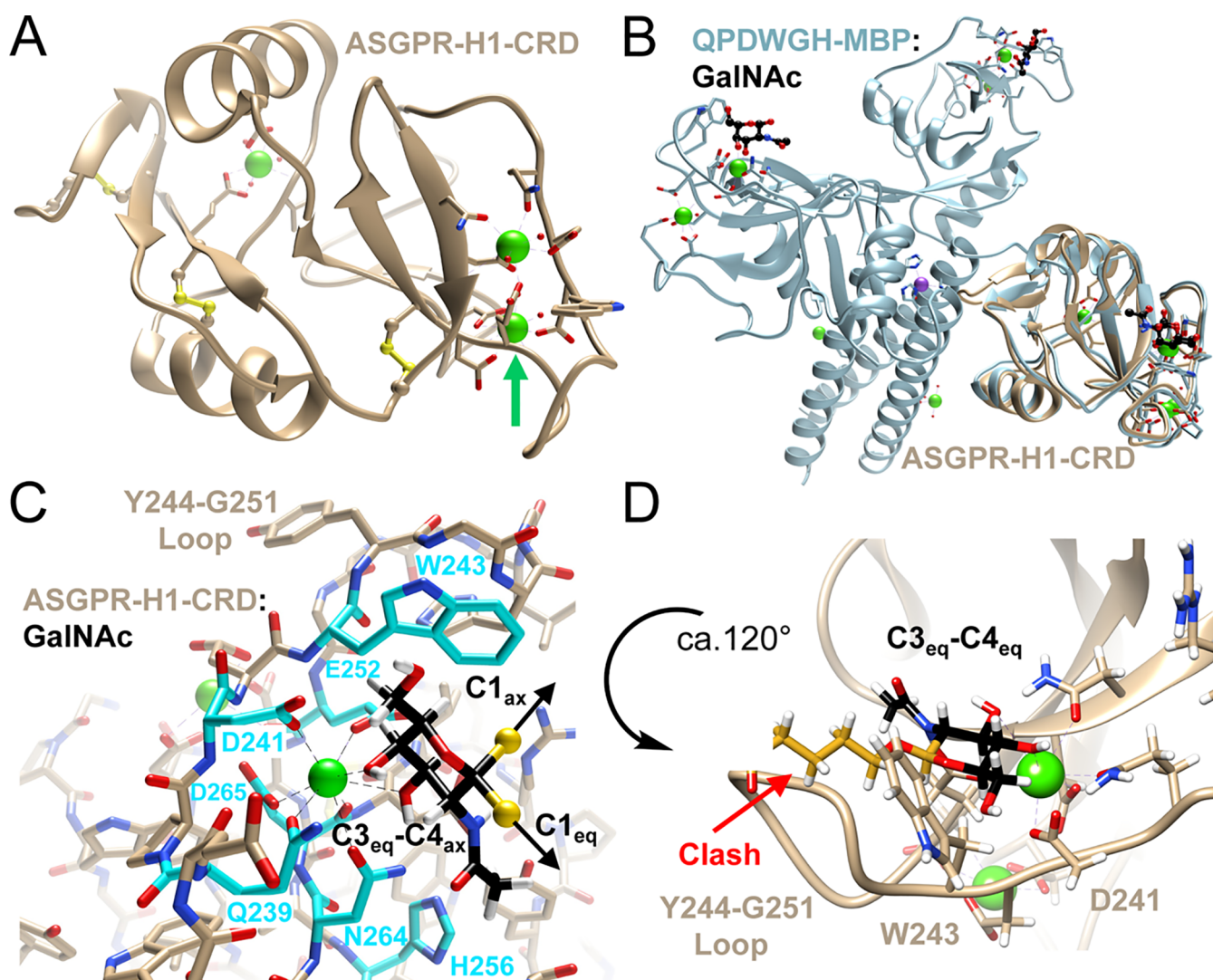
Figure 4. Modeling of the GalNAc interaction with ASGPR-CRD. (A) Crystal structure of ASGPR-H1-CRD (PDB ID 1DV8).[22] Ca^{2+} ions are in green, and their coordination spheres are indicated with dashed lines. Water molecules are shown as small red spheres. Three disulfide bridges are highlighted in the ball-and-stick mode, with sulfur atoms colored in yellow. The green arrow points to the Ca^{2+} involved in GalNAc binding. (B) Crystal structure of the trimeric mannose binding protein QPDWGH mutant (PDB ID 1BCH)[21] bound to GalNAc (light blue cartoon) with ASGPR-H1-CRD (tan) overlaid on one of the mannose binding protein lobes. GalNAc carbon atoms are shown in black, and a sodium ion coordinated to the central coil−coil stalk is colored in purple. (C) Model of GalNAc bound to ASGPR-H1-CRD based on combining the structural information from (A,B). The substituents at C1 that connect to the linker are highlighted as yellow spheres, and arrows show the directions that the linker takes for axial ($C1_{ax}$) and equatorial ($C1_{eq}$) substitutions at C1. Carbon atoms of CRD residues surrounding the GalNAc sugar are colored in cyan and labeled. The axial substitution at C1 points roughly in the direction of the six-membered ring of the W243 side chain (the shortest sulfur−ring distance is ca. 3.2 Å in the model) and may account for the differences in K_i relative to equatorial substituents that jut into open space (Table 1). (D) Changing the sugar stereochemistry from C3-equatorial/C4-axial to C3-equatorial/C4-equatorial and maintaining the coordination of the two hydroxyl groups to Ca^{2+} results in a clash between the linker and the CRD. The sugar C1 and linker carbon atoms are colored in gold, and the linker was modeled in an extended conformation. The CRD/GalNAc ($C3_{eq}−C4_{eq}$) complex model depicted in (D) is rotated by about 120° in an anti-clockwise direction around the normal to the plane of projection relative to the model of the CRD-GalNAc ($C3_{eq}−C4_{ax}$) complex model depicted in (C).

post-dose for all conjugates. Initial recovery of the TTR protein levels was observed 20 days post-dose (∼60% target reduction compared to the PBS control group). On average, the trend for target recovery was similar to the parent **I** for siRNA conjugates with anomeric linkages **II**−**VII**.

At least 80% suppression of circulating TTR protein was observed at nadir (7 days post-dose) for siRNAs conjugated to stable α and β C-glycosides linked to triantennary GalNAc (siRNAs **VII** and **VIII**), equivalent to the parent compound **I**. The siRNAs conjugated to α and β C-glycosides in the serial 1 + 1 + 1 design (siRNAs **XV** and **XVI**) yielded somewhat lower

protein reductions of approximately 70% (Figure 7), as predicted given the shorter linker design and lower ASGPR affinity. Nevertheless, no significant differences in duration of effect were observed across compounds regardless of their GalNAc ligand design.

Metabolic Stability of Novel GalNAc−siRNA Conjugates. GalNAc-conjugated siRNAs were evaluated in a previously described rat tritosome assay to evaluate their metabolic stability in the endo-lysosomal compartments.[45] The GalNAc-conjugated siRNAs were incubated in rat tritosomes at pH 5.0 for 0, 2, 6, and 24 h at 37 °C and then analyzed by
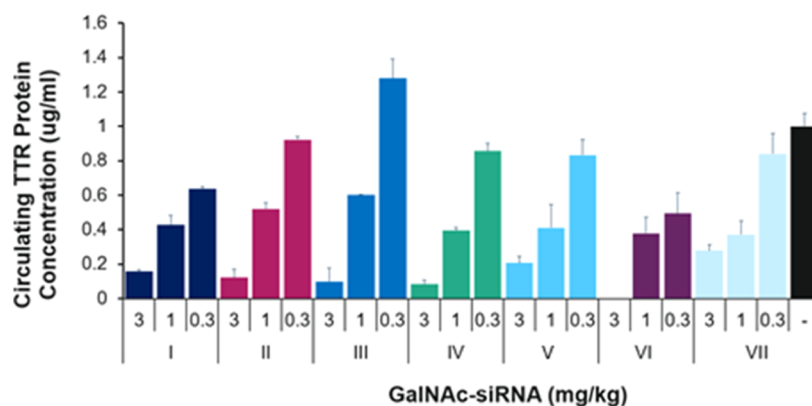
Figure 5. siRNA conjugates with anomeric linkages have activity similar to the parent in vivo. Circulating TTR levels were measured on day 7 post-dose in C57/BL6 female mice ($n = 3$). Mice were injected with a single, subcutaneous dose of 0.3, 1, or 3 mg/kg of GalNAc−siRNA or with PBS on day 0. Serum was collected on day 0 (pre-dose) and day 7 post-dose. TTR protein levels were measured and normalized to the individual pre-dose samples. Data were normalized to the saline control group. Error bars represent standard deviations.
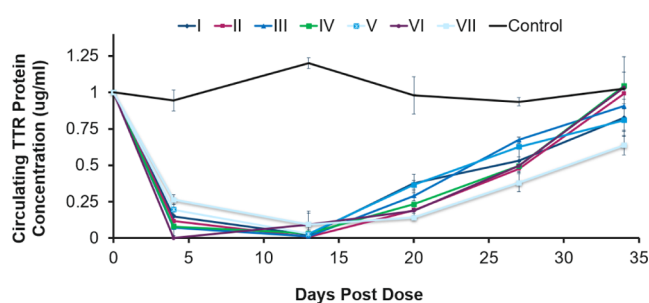
Figure 6. Durability of gene silencing by GalNAc−siRNA conjugates with stabilized anomeric linkages. Circulating TTR levels were measured over time in C57/BL6 female mice ($n = 3$) injected with a single subcutaneous dose of 3 mg/kg of GalNAc−siRNA or with PBS on day 0. Serum was collected on day 0 (pre-dose) and on days 4, 13, 20, 27, and 34 post-dose. TTR protein levels were measured and normalized to the individual pre-dose samples. Error bars represent standard deviations.

Figure 7. Pharmacodynamic profiles of TTR serum protein reduction over time for (A) triantennary GalNAc-conjugated siRNAs (**I**, **VII**, and **VIII**) or (B) 1 + 1 + 1 GalNAc-conjugated siRNAs (**XVI**, **XV**, and **IX**). Circulating TTR levels were measured over time in C57/BL6 female mice ($n = 3$) injected with a single, subcutaneous dose of 1.5 mg/kg siRNA conjugates on day 0. Serum was collected on day 0 (pre-dose) and on days 4, 13, 20, 27, and 34 post-dose. TTR protein levels were measured and normalized to the individual pre-dose samples. Error bars represent standard deviations.

analytical HPLC and by LC−MS. Carbohydrate moieties of natural beta *O*-glycosides **I** and alpha *O*-glycosides **II** were cleaved from the siRNAs within 2 h (Figure 8). As expected, GalNAc−siRNA conjugates **III−VIII** retained their sugar moieties even after 24 h in the presence of tritosomes (Figure 8).

To confirm these findings in vivo, metabolic profiles were evaluated in mouse liver either 2 or 8 h post dosing with 10 mg/kg of the GalNAc-conjugated siRNA. Livers were harvested, and sense strands were analyzed by LC−MS. As expected, the GalNAc ligand with the natural *β-O*-glycosidic linkage was cleaved from siRNA **I** at a very early time point, and no GalNAc-conjugated sense strand was detected at the 8 h time point. The *β-S-* (siRNA **III**), *β-N-* (siRNA **V**), and *α-C-* (siRNA **VII**) anomeric bonds were not cleaved at 8 h after subcutaneous administration (Figure 9). Similar stabilities were observed for siRNAs **VIII**, **XV**, and **XVI** (data not shown).

Finally, the amount of the active antisense strands in the livers of mice treated with siRNAs conjugated to modified GalNAc ligands was determined using the previously described hybridization methods.[11,12] Antisense strand levels were similar in mice treated with siRNAs conjugated to *β-S-* (siRNA **III**), *β-N-* (siRNA **V**), and *α-C-* (siRNA **VII**), and these levels were comparable to those of the siRNA conjugated to GalNAc with

the natural *β-O*-glycosidic anomeric linkage (siRNA **I**) (Figure 10). This finding indicated that the triantennary ligands described in this study do not impact loading of the antisense strand into the RNA-induced silencing complex (RISC) and that levels of the antisense strand correlate with in vivo gene silencing.
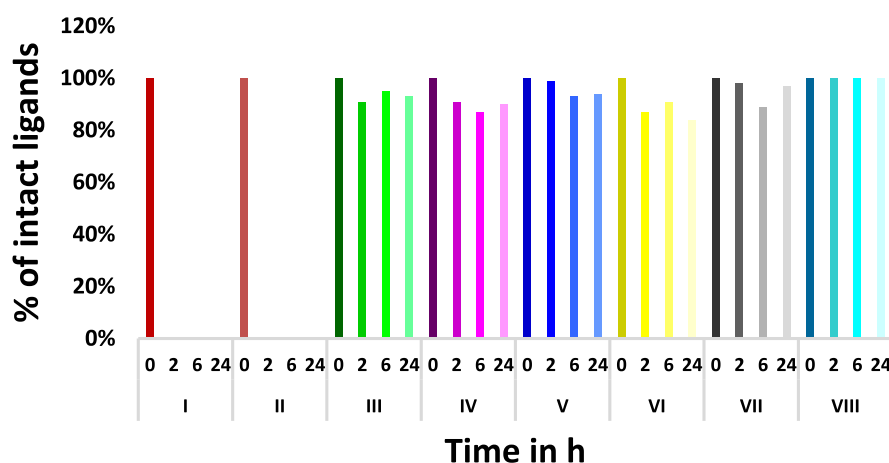
Figure 8. Modified GalNAc ligands remain on the siRNAs in rat liver tritosomes. Compounds were incubated with rat liver tritosomes for the indicated times, and the remaining full-length sense strand with the ligand was quantified by HPLC.
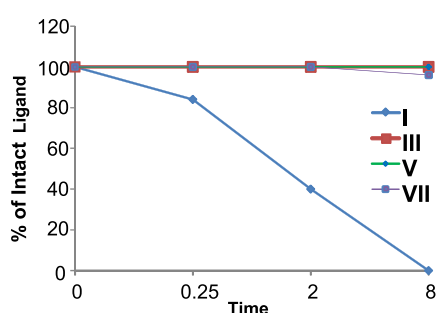
Figure 9. Anomeric linkages of modified GalNAc ligands are stable in vivo. Metabolic stability of the anomeric linkage in indicated GalNAc-conjugated siRNAs was measured at 8 h after a 10 mg/kg dose was given to C57/BL6 female mice ($n = 3$). Livers were harvested, digested, and extracted by solid-phase extraction, and the percent intact GalNAc-conjugated sense strand was analyzed by LC−MS using a Q Exactive-Orbitrap mass spectrometer.
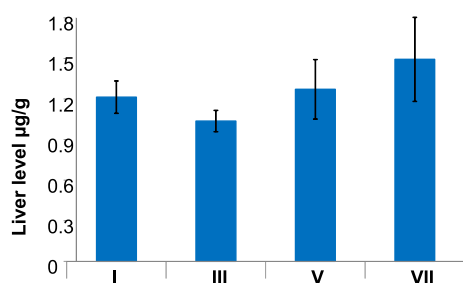
Figure 10. Antisense strand levels of siRNAs conjugated to GalNAc ligands with different anomeric linkages are similar in livers 24 h after subcutaneous dosing. The concentrations of the liver antisense strand were evaluated by hybridization methods.

■ CONCLUSIONS

In this study, we were interested in understanding the relative contributions of ASGPR-mediated uptake, glycosidases-mediated cleavage of sugar anomeric linkage, and RISC loading to the gene silencing activities of siRNAs conjugated to novel GalNAc ligands with metabolically stable linkers. As the β-*O*-glycosidic linkage is hydrolyzed by glycosidases, we reasoned that improving the metabolic stability of the natural β-*O*-glycosidic linkage against the glycosidases in the triantennary GalNAc ligand used for delivery of siRNAs into hepatocytes should improve the durability of gene silencing. The metabolic

stability enhancement expected due to the chemical changes in the anomeric linkage was confirmed in a liver tritosome assay and by analysis of intact GalNAc-conjugated sense strand in liver tissues of mice. Differences in the anomeric bond did not result in significant differences in the affinity of the GalNAc-conjugated siRNA for ASGPR, which is the receptor that facilitates efficient delivery of the GalNAc-conjugated siRNA into hepatocytes, or differences in uptake of the siRNA into hepatocytes, confirming that the receptor binding is not governed by the stereo configuration of the anomeric position and/or the nature of the anomeric linkage of the sugar moiety. Moreover, the RISC-mediated silencing efficiency was not affected by the glycosidic linkage.

Interestingly, the higher metabolic stability of the anomeric linkage did not contribute to an enhanced duration of the *Ttr* gene silencing in cell-based assays or in a mouse model. This finding indicates that the duration of RNAi activity observed in preclinical species and in humans is presumably determined by siRNA stability in endosomal and lysosomal compartments rather than by metabolic stability of the the GalNAc sugar moieties.[45] Anomeric linkage metabolic stability is not detrimental to ASGPR binding, and, more importantly, the stabilized triantennary ligands described in this study do not appear to impact loading of the antisense strand into the RISC, as silencing activity was maintained in vitro and in vivo.[40,46] In summary, the protein−nucleic acid interactions involved in the RNA metabolic stability mediated by the nucleases and RISC loading and silency efficiency mediated by the slicer enzyme Argonaute 2 appear to be more critical to the duration of action than the stability of the linkage between the GalNAc ligand and the sense strand of the siRNA. The findings from the present work further explain the ongoing efforts to improve the therapeutic utility of siRNA-GalNAc conjugates, as demonstrated by several recent publications.[47−53]

GalNAc-conjugated siRNAs such as inclisiran are now being used to treat metabolic diseases like hypercholesterolemia, which affect large numbers of patients globally, and this demands the convenient large-scale synthesis of such conjugates. As part of this study, we devised a general synthetic method to anchor the GalNAc sugar monomers to two different triantennary amine-containing oligonucleotide scaffolds, enabling rapid access to a variety of GalNAc derivative-siRNA conjugates. This post-oligonucleotide synthesis method is efficient and may prove more cost-effective

than the current on-column method.[12] This synthetic route could be used in the synthesis of GalNAc−siRNA conjugates for future therapeutic development.

■ EXPERIMENTAL SECTION

General Methods. All novel small-molecule compounds were found to be >95% pure by HPLC, NMR, and HR-MS analyses. All siRNA duplexes were purified and characterized by LC−MS and evaluated for endotoxin levels and purity levels. TLC was performed on Merck silica-coated plates. Compounds were visualized under UV light (254 nm) or after spraying with the phosphomolybdic acid staining solution, followed by heating. Flash column chromatography was performed using a Teledyne ISCO Combi Flash system and pre-packed RediSep Teledyne ISCO silica gel cartridges. All moisture-sensitive reactions were carried out under anhydrous conditions using dry glassware, anhydrous solvents, and an argon atmosphere. All commercially available reagents and solvents were purchased from Sigma-Aldrich unless otherwise stated and were used as received. ESI-MS spectra were recorded on an Agilent 6130 single quadrupole spectrometer using the direct injection mode with 0.1% acetic acid in water and methanol (1:1, v/v). ^{1}H, ^{13}C, ^{19}F, and ^{31}P NMR spectra were recorded at 400 or 500, 100 or 125, 376, and 162 MHz, respectively (Supporting Information, Section III). Chemical shifts are given in ppm with reference to the solvent residual peak (DMSO-d_6—^{1}H: δ at 2.50 ppm and ^{13}C δ at 39.5 ppm; CD$_3$OD—^{1}H: δ at 4.87 ppm and ^{13}C δ at 49.0 ppm). Coupling constants are given in Hz. Signal splitting patterns are described as singlet (s), doublet (d), triplet (t), broad signal (br s), or multiplet (m).

Compound Synthesis. *Compound 4.* To a stirred solution of acid **4A** (25.44 g, 56.9 mmol) in DCM (200 mL) were added NHS (7.2 g, 62.59 mmol), EDC (13.04 g, 68.27 mmol), and DIEA (17.6 mL, 136.5 mmol) dropwise over 5 min. The reaction mixture was stirred at room temperature for 14 h, and 100 mL of water was added, followed by extraction with DCM (100 mL twice), washing with citric acid (5%), sat. NaHCO$_3$, and brine, and drying over anhydrous Na$_2$SO$_4$. Concentration of the solvent gave the product **4** as a foamy solid (30 g, 97%). ^{1}H NMR (400 MHz, DMSO-d_6): δ 7.81 (d, J = 9.2 Hz, 1H), 5.20 (d, J = 3.3 Hz, 1H), 4.95 (dd, J = 11.2, 3.4 Hz, 1H), 4.49 (d, J = 8.5 Hz, 1H), 4.02 (s, 3H), 3.94−3.82 (m, 1H), 3.73 (dt, J = 10.6, 5.5 Hz, 1H), 3.45 (dt, J = 11.6, 5.9 Hz, 1H), 2.80 (s, 4H), 2.66 (t, J = 7.2 Hz, 2H), 2.09 (s, 3H), 1.99 (s, 3H), 1.88 (s, 3H), 1.76 (s, 3H), 1.65−1.55 (m, 4H). ^{13}C NMR (126 MHz, DMSO-d_6): δ 170.2, 170.0, 169.9, 169.6, 169.3, 168.9, 100.8, 70.5, 69.9, 68.0, 66.7, 61.4, 49.3, 40.0, 39.8, 39.7, 39.5, 39.3, 39.2, 39.0, 29.8, 27.8, 25.4, 22.7, 20.9, 20.5, 20.4. HRMS calcd for C$_{23}$H$_{33}$N$_2$O$_{13}$ [M + H]$^{+}$, 545.1983; found, 545.1985.

Compound 16A. Solid sodium periodate (3.44 g, 16 mmol) was added to a stirred mixture of alkene **16B** synthesized as described previously[12] (1.26 g, 2.93 mmol) in DCM (10 mL), acetonitrile (10 mL), and water (15 mL), followed by the addition of ruthenium trichloride monohydrate (15 mg, 0.053 mmol). Change of color from light to dark green and a slight exothermic effect indicated the initiation of the oxidation reaction. The mixture was stirred at ambient temperature and monitored by TLC. After 3 h, the mixture was filtered through a plug of Celite and washed with DCM. Solvents were removed under reduced pressure, and the residue was dissolved in DCM (50 mL), washed with water (50 mL) and brine (50 mL), and dried over anhydrous Na$_2$SO$_4$. Solvents were removed under vacuum, and purification by column chromatography using 20−100% ethyl acetate in hexanes as eluents yielded compound **16A** (0.98 g, 77%) as a colorless viscous oil. ^{1}H NMR (400 MHz, DMSO-d_6): δ 12.02 (br s, 1H), 7.99 (d, J = 8.1 Hz, 1H), 5.31 (d, J = 2.5 Hz, 1H), 5.0 (dd, J = 11.8, 3.2 Hz, 1H), 4.83 (d, J = 3.5 Hz, 1H), 4.27−4.09 (m, 2H), 4.06−3.95 (m, 2H), 3.70−3.53 (m, 1H), 3.48−3.34 (m, 1H), 2.30−2.17 (m, 2H), 2.09 (s, 3H), 1.99 (s, 3H), 1.89 (s, 3H), 1.80 (s, 3H), 1.64−1.50 (m, 4H). ^{13}C NMR (126 MHz, DMSO-d_6): δ 174.3, 170.0, 169.9, 169.7, 169.6, 96.8, 67.4, 67.3, 67.1, 66.0, 61.9, 47.2, 33.3, 28.3, 22.3, 21.1, 20.5, 20.48, 20.42. HRMS calcd for C$_{19}$H$_{30}$NO$_{11}$ [M + H]$^{+}$, 448.1819; found, 448.1828.

Compound 16. To a solution of **16A** (171 mg, 0.38 mmol) in anhydrous DCM (10 mL) was added N-hydroxysuccinimide (NHS) (70 mg, 0.57 mmol) and DIEA (0.20 mL, 1.14 mmol). EDC (110 mg, 0.57 mmol) was added, and the reaction was stirred overnight at ambient temperature. The reaction mixture was extracted with DCM, followed by washing with water (50 mL) and brine (50 mL), and the organic layer was dried over anhydrous Na$_2$SO$_4$. Solvents were removed under vacuum, and purification by column chromatography using EtOAc/hexanes (30−100%) as eluents yielded **16** as a white foam (0.172 g, 82%). ^{1}H NMR (400 MHz, DMSO-d_6): δ 8.00 (d, J = 8.1 Hz, 1H), 5.31 (dd, J = 3.4, 1.3 Hz, 1H), 5.01 (dd, J = 11.8, 3.2 Hz, 1H), 4.85 (d, J = 3.5 Hz, 1H), 4.27−4.08 (m, 2H), 4.09−3.93 (m, 2H), 3.63 (dt, J = 9.9, 5.9 Hz, 1H), 3.42 (dt, J = 10.0, 5.9 Hz, 1H), 2.80 (s, 4H), 2.70 (t, J = 7.2 Hz, 2H), 2.09 (s, 3H), 1.99 (s, 3H), 1.89 (s, 3H), 1.80 (s, 3H), 1.77−1.56 (m, 4H). ^{13}C NMR (126 MHz, DMSO-d_6): δ 170.0, 169.8, 169.7, 169.57, 169.52, 168.7, 96.7, 67.4, 67.0, 66.8, 65.9, 61.7, 47.1, 29.7, 27.6, 25.3, 22.2, 20.94, 20.4, 20.3, 20.2. HRMS calcd for C$_{23}$H$_{33}$N$_2$O$_{13}$ [M + H]$^{+}$, 545.1983; found, 545.1987.

Compound 17B. To a stirred solution of **17D** (1.65 g, 5 mmol) in ethylene dichloride (15 mL) were added *tert*-butyl 5-mercaptopentanoate **17C** (1.0 g, 5.25 mmol) and TMSOTf (0.181 mL, 1.0 mmol) at 0 °C, and the mixture was stirred at room temperature overnight. The reaction mixture was diluted with CH$_2$Cl$_2$ (100 mL) followed by washing with water (50 mL), saturated aq. NaHCO$_3$ (50 mL), brine (50 mL), and the organic layer was dried over anhydrous Na$_2$SO$_4$. Concentration of the solvent gave the crude material, which was purified by column chromatography (0−5% MeOH in CH$_2$Cl$_2$) to give **17B** (380 mg, 0.731 mmol, 15%) as white foam. ^{1}H NMR (400 MHz, CDCl$_3$): δ 5.55 (d, J = 9.6 Hz, 1H), 5.38 (d, J = 3.2 Hz, 1H), 5.12 (dd, J = 10.8, 3.2 Hz, 1H), 4.61 (d, J = 10.4 Hz, 1H), 4.24 (q, J = 10.2 Hz, 1H), 4.08−4.18 (m, 2H), 3.90 (t, J = 6.6 Hz, 1H), 2.75−2.80 (m, 1H), 2.64−2.69 (m, 1H), 2.23−2.27 (m, 2H), 2.16 (s, 3H), 2.05 (s, 3H), 2.01 (s, 3H), 1.96 (s, 3H), 1.61−1.69 (m, 4H), 1.45 (s, 9H). ^{13}C NMR (100 MHz, CDCl$_3$): δ 173.1, 170.8, 170.6, 170.5, 170.4, 84.9, 80.5, 74.6, 71.6, 67.1, 61.8, 49.8, 35.0, 29.9, 28.8, 28.3, 23.9, 23.5, 20.9, 20.8. HRMS calcd for C$_{23}$H$_{37}$NNaO$_{10}$S [M + Na]$^{+}$, 542.2036; found, 542.2032.

Compound 17. To a stirred solution of compound **17B** (380 mg, 0.731 mmol) in CH$_2$Cl$_2$ (4 mL) was added trifluoroacetic acid (1 mL) at 0 °C. The mixture was stirred at 0 °C for 2 h and then at room temperature for 3 h. The solvent was removed by evaporation, and the residue was co-evaporated with toluene to obtain the crude acid. This material in CH$_2$Cl$_2$ (5 mL) was added to N-hydroxysuccinimide (168 mg, 1.46 mmol), EDC (280 mg, 1.46 mmol), and DIEA (0.764 mL, 4.38 mmol), and the reaction mixture was stirred at room temperature for 14 h. The reaction mixture was diluted with CH$_2$Cl$_2$ (100 mL), followed by washing with water (50 mL), saturated aq. NaHCO$_3$ (50 mL), and brine (50 mL). The organic layer was dried over anhydrous Na$_2$SO$_4$. Concentration of the solvent gave the crude material, which was purified by column chromatography (0−5% MeOH in CH$_2$Cl$_2$) to give **17** (284 mg, 0.507 mmol, 69%) as a white foam. ^{1}H NMR (400 MHz, CDCl$_3$): δ 5.70 (d, J = 9.6 Hz, 1H), 5.36 (d, J = 3.2 Hz, 1H), 5.08 (dd, J = 10.4, 3.2 Hz, 1H), 4.60 (d, J = 10.8 Hz, 1H), 4.32 (q, J = 10.2 Hz, 1H), 4.11−4.14 (m, 2H), 3.93 (t, J = 6.6 Hz, 1H), 2.85−2.90 (m, 4H), 2.51−2.74 (m, 4H), 2.16 (s, 3H), 2.04 (s, 3H), 1.99 (s, 3H), 1.95 (s, 3H), 1.76−1.79 (m, 4H). ^{13}C NMR (125 MHz, CDCl$_3$): δ 170.9, 170.6, 170.5, 170.4, 169.7, 168.9, 84.3, 74.5, 71.7, 67.1, 61.9, 49.4, 30.8, 29.4, 28.0, 25.8, 25.7, 23.5, 23.4, 20.92, 20.88, 20.86. HRMS calcd for C$_{23}$H$_{32}$N$_2$NaO$_{12}$S [M + Na]$^{+}$, 583.1574; found, 583.1572.

Compound 18. To a solution of compound **18A**[39] (2.40 g, 5.18 mmol) in CH$_2$Cl$_2$ (30 mL) were added N-hydroxysuccinimide (716 mg, 6.22 mmol), EDC (1.19 g, 6.22 mmol), and DIEA (2.7 mL, 15.5 mmol), and the reaction mixture was stirred at room temperature for 14 h. The reaction mixture was diluted with CH$_2$Cl$_2$ (100 mL), followed by washing with water (50 mL), saturated aq. NaHCO$_3$ (50 mL), and brine (50 mL). The organic layer was dried over anhydrous Na$_2$SO$_4$. Concentration of the solvent gave the crude material, which was purified by column chromatography (0−5% MeOH in CH$_2$Cl$_2$)

to give **18** (1.83 g, 3.26 mmol, 63%) as a white foam. ^{1}H NMR (500 MHz, CDCl$_3$): δ 5.60 (d, J = 8.5 Hz, 1H), 5.49 (d, J = 5.5 Hz, 1H), 5.38 (d, J = 2.0 Hz, 1H), 5.04 (dd, J = 11.8 Hz, 3.3 Hz, 1H), 4.74–4.80 (m, 1H), 4.54 (t, J = 6.5 Hz, 1H), 4.12 (dd, J = 11.3 Hz, 6.3 Hz, 1H), 4.07 (dd, J = 11.3 Hz, 6.8 Hz, 1H), 2.84 (br s, 4H), 2.58–2.72 (m, 4H), 2.16 (s, 3H), 2.04 (s, 3H), 2.00 (s, 3H), 1.97 (s, 3H), 1.73–1.84 (m, 4H). ^{13}C NMR (125 MHz, CDCl$_3$): δ 171.1, 170.5, 170.4, 170.3, 169.3, 168.3, 85.0, 68.7, 67.5, 62.0, 48.4, 30.59, 30.57, 28.5, 25.7, 23.7, 23.5, 20.88, 20.86. HRMS calcd for C$_{23}$H$_{32}$N$_2$NaO$_{12}$S [M + H]$^+$, 583.1574; found, 583.1566.

Compound 19. To a stirred solution of 2,3,4,6-tetra-*O*-acetyl-β-D-galactopyranosylamine **19B** (10.0 g, 28.89 mmol) and glutaric anhydride (3.29 g, 28.89 mmol) in DCM (100 mL) were added pyridine (4.6 g) and DMAP (0.176 g). The reaction mixture was stirred for 14 h at room temperature. Concentration followed by drying under reduced pressure gave the crude product acid **19A** (11.45 g, 86%). To a stirred solution of the acid (7.6 g, 16.51 mmol) in DCM (100 mL) were added NHS (2.09 g, 18.16 mmol), EDC (3.8 g, 19.8 mmol), and DIEA (7.16 mL, 41.27 mmol) dropwise over 5 min. The reaction mixture was stirred at room temperature for 14 h, and 100 mL of water was added, followed by extraction with DCM (50 mL twice), washing with citric acid (5%), sat. NaHCO$_3$, and brine, and drying over anhydrous Na$_2$SO$_4$. Concentration of the solvent gave the product **19** (6 g, 65%) as a foamy solid. ^{1}H NMR (400 MHz, CDCl$_3$): δ 7.07 (d, J = 8.6 Hz, 1H), 5.83 (d, J = 8.8 Hz, 1H), 5.09 (t, J = 9.2 Hz, 1H), 5.01 (dd, J = 5.02, 11.2 Hz, 1H), 4.3 (q, J = 9.91 Hz, 1H), 4.17–4.05 (m, 2H), 3.99 (t, J = 6.6 Hz, 1H), 2.85 (br s, 4H), 2.65 (t, J = 7.14 Hz, 2H), 2.43–2.3 (m, 2H), 2.16 (s, 3h), 2.04 (s, 3H), 2.03 (s, 3H), 2.1–1.98 (m, 2H), 1.94 (s, 3H). ^{13}C NMR (101 MHz, CDCl$_3$): δ 172.5, 172.2, 171.0, 170.5, 170.2, 168.2, 80.0, 72.2, 70.9, 66.6, 61.5, 49.3, 34.6, 30.0, 25.7, 23.1, 20.7, 20.3. HRMS calcd for C$_{23}$H$_{31}$N$_3$O$_{13}$ [M + H]$^+$, 558.1935; found, 558.1890.

Compound 20D. To a stirred solution of 2,3,4,6-tetra-*O*-acetyl-β-D-galactopyranosylamine **19B** (3.0 g, 8.66 mmol) in acetonitrile (50 mL) was added *N,N′*-disuccinimidyl carbonate (2.22 g, 8.66 mmol). After stirring overnight (14 h) at room temperature, the mixture was concentrated, extracted with ethyl acetate (50 mL three times), washed with water, 5% citric acid, and brine, and dried over anhydrous Na$_2$SO$_4$. Removal of the solvent under reduced pressure gave the product **20D** (3.8 g, 95%). ^{1}H NMR (400 MHz, DMSO-d_6): δ 9.21 (d, J = 9.28 Hz, 1H), 7.91 (d, J = 8.96 Hz, 1H), 5.26 (d, J = 3.32, 1H), 5.07 (dd, J = 3.5, 11.0 Hz, 1H), 4.95 (t, J = 9.48 Hz, 1H), 4.13 (t, J = 6.28 Hz, 1H), 4.09–3.96 (m, 3H), 2.76 (br s, 4H), 2.09 (s, 3H), 1.99 (s, 3H), 1.89 (s, 3H), 1.79 (s, 3H). ^{13}C NMR (101 MHz, DMSO-d_6): δ 172.8, 171.3, 170.6, 170.0, 169.8, 169.50, 81.7, 71.5, 70.6, 66.6, 61.6, 48.6, 25.3, 22.6, 20.5, 20.48, 20.45. HRMS calcd for C$_{19}$H$_{25}$N$_3$NaO$_{12}$ [M + Na]$^+$, 510.1336; found, 510.1333.

Compound 20B. To a stirred solution of **20D** (0.663 g, 1.36 mmol) in DCM (15 mL) were added *p*-toluenesulfonate salt of β-alanine benzyl ester **20C** (0.526 g, 1.5 mmol) and triethylamine (0.4 mL). The reaction mixture was stirred overnight (14 h) at room temperature. Concentration of the solvent was followed by extraction with ethyl acetate (25 mL ×3), washing with water, 10% citric acid, sat. NaHCO$_3$, and brine, and drying over anhydrous Na$_2$SO$_4$. Concentration of the solvent gave the product **20B** (0.7 g, 80%). ^{1}H NMR (400 MHz, CDCl$_3$): δ 7.4–7.3 (m, 5H), 6.04 (d, J = 8.64 Hz, 1H), 5.96 (d, J = 8.04 Hz, 1H), 5.38–5.34 (m, 1H), 5.32–5.22 (m, 1H), 5.12 (br s, 2H), 5.05 (dd, J = 2.86, 11.22 Hz, 1H), 4.98 (t, J = 9.0, 1H), 4.28 (q, J = 9.85 Hz, 1H), 4.2–4.04 (m, 2H), 3.97 (t, J = 6.52 Hz, 1H), 3.55–3.35 (m, 2H), 2.6–2.5 (m, 2H), 2.15 (s, 3H), 2.03 (s, 3H), 1.94 (s, 3H). ^{13}C NMR (126 MHz, CDCl$_3$): δ 171.4, 169.91, 169.9, 169.8, 169.5, 156.7, 136.1, 128.4, 128.0, 127.9, 80.7, 71.1, 70.6, 66.6, 65.5, 61.5, 48.0, 35.2, 34.6, 22.7, 20.5, 20.4. HRMS calcd for C$_{25}$H$_{33}$N$_3$NaO$_{11}$ [M + Na]$^+$, 574.2013; found, 574.1949.

Compound 20. To a stirred solution of **20B** (0.7 g, 1.26 mmol) in EtOH (15 mL) was added Pd/C (0.1 g), and the reaction was stirred under hydrogen atmosphere overnight (14 h). The catalyst was removed by filtration over Celite, and the product was washed with EtOH (950 mL) and concentrated to yield the corresponding carboxylic acid, which was used for the next step without purification.

To a stirred solution of the carboxylic acid thus obtained in DCM (20 mL) were added EDC (488 mg, 2.56 mmol), NHS (730 mg, 6.35 mmol), and DIEA (0.88 mL, 5.07 mmol), and the reaction mixture was stirred overnight. Concentration of the reaction mixture followed by column chromatography gave **20** (250 mg, 35%). ^{1}H NMR (400 MHz, CDCl$_3$): δ 6.37 (s, 1H), 6.01 (s, 1H), 5.81 (s, 1H), 5.35 (d, J = 3.28 Hz, 1H), 5.05 (dd, J = 3.58 Hz, 11.04 Hz, 1H), 5.0 (t, J = 9.1 Hz, 1H), 4.23 (q, J = 10.48 Hz, 1H), 4.15–4.05 (m, 2H), 3.99 (t, J = 6.7 Hz, 1H), 3.7–3.46 (m, 2H), 2.9–2.73 (m, 6H), 2.14 (s, 3H), 2.02 (s, 3H), 2.06 (s, 3H), 1.93 (s, 3H). ^{13}C NMR (101 MHz, DMSO-d_6): δ 169.4, 166.4, 166.3, 166.0, 165.2, 163.1, 153.6, 76.8, 67.5, 66.3, 62.2, 57.1, 45.5, 31.4, 27.6, 21.3, 21.1, 18.6, 16.4, 16.38. HRMS calcd for C$_{22}$H$_{31}$N$_4$O$_{13}$ [M + H]$^+$, 559.1888; found, 559.1890.

Compound 21A. To a stirred solution of compound **21B** (1.94 g, 5.22 mmol) in CH$_2$Cl$_2$ (20 mL) were added benzyl 4-pentenoate (2.99 g, 15.7 mmol) and second generation Grubb's catalyst (433 mg, 0.522 mmol), and the reaction mixture was heated at 40 °C for 40 h. The solvent was removed, and the residue was passed through a short silica gel chromatography column and concentrated under reduced pressure. To a solution of the crude product in EtOAc (30 mL) was added palladium on carbon (10 wt %, Degussa type E101 NE/W: 185 mg). The reaction mixture was stirred under H$_2$ atmosphere for 14 h. After filtration over a Celite bed and evaporation of the solvent, the residue was purified by column chromatography (0–5% MeOH in CH$_2$Cl$_2$) to give compound **21A** (903 mg, 2.03 mmol, 39%). ^{1}H NMR (500 MHz, CDCl$_3$): δ 5.89 (d, J = 8.5 Hz, 1H), 5.31 (t, J = 3.0 Hz, 1H), 5.13 (dd, J = 9.5 Hz, 3.0 Hz, 1H), 4.44–4.48 (m, 1H), 4.28 (br s, 1H), 4.19–4.21 (m, 1H), 4.09 (dd, J = 11.5 Hz, 5.0 Hz, 1H), 4.00–4.02 (m, 1H), 2.35 (t, J = 7.3 Hz, 2H), 2.11 (s, 3H), 2.05 (s, 6H), 1.99 (s, 3H), 1.63 (t, J = 7.3 Hz, 2H), 1.32–1.44 (m, 6H). ^{13}C NMR (125 MHz, CDCl$_3$): δ 178.2, 171.1, 170.8, 170.5, 170.3, 72.0, 68.8, 68.5, 67.1, 61.6, 49.2, 33.8, 28.8, 26.1, 25.1, 24.6, 23.3, 21.0, 20.89, 20.85. HRMS calcd for C$_{20}$H$_{31}$NNaO$_{10}$ [M + Na]$^+$, 468.1846; found, 468.1849.

Compound 21. To a stirred solution of compound **21A** (326 mg, 0.732 mmol) in CH$_2$Cl$_2$ (5 mL) were added *N*-hydroxysuccinimide (127 mg, 1.10 mmol), EDC (211 mg, 1.10 mmol), and DIEA (0.383 mL, 2.20 mmol), and the reaction mixture was stirred at room temperature for 14 h. The reaction mixture was diluted with CH$_2$Cl$_2$ (50 mL), followed by washing with water (50 mL), saturated aq. NaHCO$_3$ (50 mL), and brine (50 mL), and the organic layer was dried over anhydrous Na$_2$SO$_4$. After concentration of the solvent, the crude material was purified by column chromatography (0–5% MeOH in CH$_2$Cl$_2$) to give **21** (300 mg, 0.553 mmol, 76%) as a white foam. ^{1}H NMR (500 MHz, CDCl$_3$): δ 5.70 (d, J = 8.5 Hz, 1H), 5.30 (t, J = 3.0 Hz, 1H), 5.12 (dd, J = 9.5 Hz, 3.0 Hz, 1H), 4.44–4.48 (m, 1H), 4.25 (br s, 1H), 4.18–4.21 (m, 1H), 4.09 (dd, J = 11.5 Hz, 5.0 Hz, 1H), 3.98–4.01 (m, 1H), 2.84 (br s, 4H), 2.61 (t, J = 7.3 Hz, 2H), 2.11 (s, 3H), 2.050 (s, 3H), 2.045 (s, 3H), 1.98 (s, 3H), 1.73–1.78 (m, 2H), 1.32–1.49 (m, 6H). ^{13}C NMR (125 MHz, CDCl$_3$): δ 171.0, 170.7, 170.3, 170.2, 169.4, 168.6, 71.9, 68.8, 68.4, 68.3, 67.1, 61.7, 49.1, 30.9, 28.4, 26.1, 25.7, 25.6, 25.0, 24.9, 24.5, 24.3, 23.4, 23.3, 21.0, 20.90, 20.85. HRMS calcd for C$_{24}$H$_{34}$N$_2$NaO$_{12}$ [M + H]$^+$, 565.2016; found, 565.2007.

Compound 22D. To a solution of compound **22E** (4.20 g, 8.32 mmol) in dry THF (83 mL) at 0 °C was added 1 M LiAlH$_4$ solution in THF (16.5 mL) dropwise. The reaction mixture was slowly brought to room temperature and stirred for 1 h. The reaction mixture was then cooled to 0 °C. EtOAc and water were added, and the solution was neutralized with 1 N NaOH and then stirred for 15 min. The insoluble white precipitate was removed by filtration through a Celite pad, and the filtrate was extracted with EtOAc. The organic layer was washed with brine and dried over anhydrous Na$_2$SO$_4$. Solvent and volatiles were removed under vacuum to obtain a crude amine that was dissolved in dry pyridine and treated with Ac$_2$O (943 μL, 9.98 mmol) in the presence of DMAP (102 mg, 0.832 mmol) at room temperature for 5 h with stirring. The reaction mixture was diluted with DCM and then quenched excess Ac$_2$O with saturated aq. NaHCO$_3$. The organic layer was isolated and washed with brine. The solvent was removed under vacuum. The crude

residue was purified by column chromatography on silica gel (EtOAc/hexanes 50−100%) to afford **22D** (1.08 g, 25%) as a white solid. ^{1}H NMR (400 MHz, CDCl$_3$): δ 7.38−7.23 (m, 15H), 5.84 (ddd, J = 17.3, 10.4, 7.1 Hz, 1H), 5.29−5.12 (m, 3H), 4.91 (d, J = 11.6 Hz, 1H), 4.66 (dd, J = 27.6, 11.8 Hz, 2H), 4.56−4.37 (m, 3H), 4.13−3.96 (m, 2H), 3.93−3.76 (m, 2H), 3.70−3.54 (m, 3H), 1.87 (s, 3H). ^{13}C NMR (126 MHz, CDCl$_3$): δ 173.9, 170.4, 138.8, 138.3, 138.1, 135.5, 134.2, 128.8, 128.7, 128.66, 128.62, 128.5, 128.42, 128.40, 128.27, 128.23, 128.19, 128.14, 128.08, 128.00, 127.9, 127.8, 119.9, 118.9, 82.5, 81.10, 80.11, 79.6, 77.5, 77.4, 77.22, 77.15, 77.07, 76.97, 74.90, 74.8, 73.8, 73.7, 72.8, 72.3, 71.7, 69.0, 68.8, 55.6, 53.1, 29.9, 23.9, 21.4. HRMS calcd for [M + Na]$^+$ C$_{31}$H$_{35}$NO$_5$Na, 524.2407; found, 524.2415.

Compound 22C. A round-bottom flask was charged with 2nd generation Grubbs catalyst (213 mg, 0.251 mmol, 10 mol %), and compound **22D** (1.26 g, 2.51 mmol) was added. The system was flushed with Ar three times. Dry DCM (25 mL) was added, followed by a solution of *tert*-butyl hex-5-enoate (1.28 g, 7.53 mmol) in dry DCM (15 mL) dropwise. The resulting mixture was stirred for 6 h at 40 °C. The solvent was removed under vacuum. The crude residue was purified by column chromatography on silica gel (EtOAc/hexanes 50−100%) to afford compound **22C** (1.10 g, 68%) as a white foam. ^{1}H NMR (400 MHz, CDCl$_3$): δ 7.50−7.05 (m, 15H), 5.64 (ddd, J = 15.3, 7.5, 6.1 Hz, 1H), 5.47 (ddd, J = 15.5, 7.7, 1.5 Hz, 1H), 5.26 (d, J = 7.9 Hz, 1H), 4.91 (d, J = 11.7 Hz, 1H), 4.65 (dd, J = 28.0, 11.8 Hz, 2H), 4.46 (dd, J = 11.9, 6.9 Hz, 3H), 4.14 (d, J = 7.9 Hz, 1H), 4.08−3.94 (m, 2H), 3.94−3.76 (m, 2H), 3.69−3.42 (m, 4H), 2.24−2.11 (m, 2H), 2.11−1.81 (m, 6H), 1.75−1.53 (m, 5H), 1.50−1.01 (m, 12H). ^{13}C NMR (101 MHz, CDCl$_3$): δ 173.8, 173.7, 173.1, 170.4, 170.3, 156.9, 138.91, 138.86, 138.6, 138.4, 138.1, 138.0, 137.6, 135.9, 135.0, 134.9, 131.1, 128.8, 128.7, 128.63, 128.59, 128.5, 128.44, 128.38, 128.20, 128.18, 128.1, 128.0, 127.9, 127.70, 127.67, 127.0, 82.5, 81.0, 80.6, 80.3, 79.9, 79.5, 78.2, 77.6, 77.4, 77.2, 77.1, 76.9, 74.8, 74.73, 74.66, 74.6, 73.72, 73.68, 72.8, 72.6, 72.2, 71.7, 71.6, 68.9, 68.8, 55.7, 53.3, 52.3, 49.3, 35.0, 34.8, 34.2, 31.8, 31.7, 28.3, 27.3, 25.8, 25.2, 24.5, 24.4, 23.8, 23.7, 21.4. HRMS calcd for C$_{39}$H$_{50}$NO$_7$ [M+H]$^+$, 644.3587; found, 644.3583.

Compound 22B. To the solution of compound **22C** (1.10 g, 1.71 mmol) in EtOH (17 mL) was added 10 wt % Pd−C (1.1 g). The mixture was stirred under a H$_2$ atmosphere at room temperature for 12 h. After completion of the reaction, the mixture was filtered through a Celite pad, washed with EtOH, and the filtrate was concentrated to obtain the tri-hydroxy compound. Acetylation of this tri-hydroxy compound was done with Ac$_2$O (553 μL, 8.55 mmol), in the presense of DMAP (21.0 mg, 0.171 mmol) in anhydrous pyridine (17 mL) at room temperature under stirring for 5 h. The standard workup gave a crude product that was subsequently purified by column chromatography on silica gel (0−5% MeOH in CH$_2$Cl$_2$) to afford compound **22B** (814 mg, 95%) as a white foam. ^{1}H NMR (400 MHz, CDCl$_3$): δ 5.39 (d, J = 9.7 Hz, 1H), 5.33 (dd, J = 3.4, 1.1 Hz, 1H), 4.93 (dd, J = 10.9, 3.4 Hz, 1H), 4.22−4.01 (m, 3H), 3.77 (td, J = 6.7, 1.2 Hz, 1H), 3.26−3.15 (m, 1H), 2.16 (d, J = 16.2 Hz, 5H), 2.07−1.89 (m, 9H), 1.64−1.45 (m, 5H), 1.42 (s, 9H); 1.35−1.19 (m, 3H). ^{13}C NMR (126 MHz, CDCl$_3$): δ 173.4, 171.3, 170.7, 170.6, 170.4, 80.2, 80.0, 77.5, 77.4, 77.2, 77.0, 74.2, 72.3, 67.4, 62.0, 60.6, 50.4, 35.62, 35.58, 34.7, 31.7, 31.5, 29.0, 28.9, 28.31, 28.30, 25.31, 25.27, 25.2, 25.11, 25.07, 25.02, 24.9S, 23.6, 22.0, 21.2, 21.0, 20.94, 20.89, 14.4. HRMS calcd for C$_{24}$H$_{39}$NO$_{10}$Na [M + Na]$^+$, 524.2472; found, 524.2493.

Compound 22. To the solution of compound **22B** (800 mg, 1.60 mmol) in CH$_2$Cl$_2$ (16 mL) was added TFA (4 mL) dropwise. The mixture was stirred at room temperature for 5 h. After completion of deprotection, the volatiles were removed under vacuum. The resultant residue was co-evaporated with toluene three times and then dissolved in dry CH$_2$Cl$_2$ (16 mL). To the solution of the carboxylic acid **22A** thus obtained were added NHS (276 mg, 2.40 mmol), EDC (373 mg, 2.40 mmol), and DIEA (836 μL, 4.80 mmol). The reaction mixture was stirred for 12 h. The standard workup gave a crude product that was purified by column chromatography on silica gel (0−5% MeOH in CH$_2$Cl$_2$) to afford compound **22** (540 mg, 63% in 2

steps) as a white foam. ^{1}H NMR (400 MHz, CDCl$_3$): δ 5.57 (d, J = 10.0 Hz, 1H), 5.31 (d, J = 3.2 Hz, 1H), 4.92 (dd, J = 11.2, 3.2 Hz, 1H), 4.20−4.00 (m, 3H), 3.82−3.74 (m, 1H), 3.31−3.19 (m, 1H), 2.83 (s, 4H), 2.59 (t, J = 7.2 Hz, 2H), 2.13 (s, 3H), 2.02 (s, 3H), 1.97 (s, 3H), 1.92 (s, 3H), 1.82−1.30 (m, 8H). ^{13}C NMR (126 MHz, CDCl$_3$): δ 171.2, 170.60, 170.55, 170.4, 169.5, 168.8, 79.1, 74.1, 72.2, 67.3, 62.0, 50.1, 31.04, 31.02, 28.0, 25.7, 24.6, 24.5, 23.4, 20.90, 20.87, 20.8. HRMS calcd for C$_{24}$H$_{35}$N$_2$O$_{12}$ [M + H]$^+$, 543.2190; found, 543.2190.

Compound 8. To a stirred solution of amine **5** (80.18 g, 158.7 mmol), mono acid **6** (48.4 g, 198.36 mmol), and HOBt (32.17 g, 238.3 mmol) in dichloromethane (DCM; 1 L) and DMF (100 mL) was added *N*-((3-(dimethylaminopropyl))-*N*′-ethylcarbodiimide hydrochloride (37.9 g, 198.4 mmol) portionwise over 15 min. To this solution was added DIEA (69 mL, 396.7 mmol) dropwise over 30 min. After stirring at room temperature for 2 days, 100 mL of water was added, and the volatile DCM was removed. To the DMF/water mixture was added 1 L of water, and the mixture was left at room temperature until it separated into two layers. The turbid water/DMF layer was decanted and carefully washed with 100 mL of water; this procedure was repeated twice. The obtained viscous oil was dissolved in DCM (500 mL) and washed with water (500 mL), 10% citric acid (500 mL), sat. NaHCO$_3$ (250 mL), and brine (200 mL) and dried over Na$_2$SO$_4$. Concentration of the solvent gave **7** (120 g) as a pale yellow oil, and this material was dissolved in 1 L of 95% formic acid and stirred at room temperature for 2 days. The formic acid was concentrated under reduced pressure, followed by co-evaporation with toluene (2× 500 mL), and dried under high vacuum overnight to yield **8** (89.4 g) as white solid. ^{1}H NMR (400 MHz, DMSO-d_6): δ 12.13 (br s, 3H), 6.89 (s, 1H), 3.57 (s, 6H), 3.55 (s, 6H), 3.53 (s, 3H), 2.41 (t, J = 6.2 Hz, 6H), 2.27 (t, J = 7.3 Hz, 2H), 2.03 (t, J = 7.2 Hz, 2H), 1.55−1.35 (m, 4H), 1.22 (s, 12H). ^{13}C NMR (126 MHz, DMSO-d_6): δ 173.3, 172.5, 172.47, 68.3, 66.7, 59.6, 51.1, 35.9, 34.6, 33.3, 28.9, 28.84, 28.8, 28.6, 28.5, 28.47, 25.3, 24.5. HRMS calcd for C$_{26}$H$_{46}$NO$_{12}$ [M + H]$^+$, 564.3020; found, 564.3015.

Compound 10. To a stirred solution of **8** (89.5 g, 158.7), amine **9** (103.6 g, 595 mmol), EDC·HCl (113.7 g, 595 mmol), and HOBt (96.4 g, 630 mmol) in DCM/DMF (1.5 L/0.5 L) was added DIEA (207.4 mL, 1190 mmol) dropwise over 10 min. The solution was stirred at room temperature for 14 h, and then 100 mL of water was added. The DCM was removed by evaporation under reduced pressure. Another 1 L of water was added, the water layer was carefully removed, and this procedure was repeated twice. The obtained viscous oil was dissolved in DCM (500 mL), washed with water (500 mL), 10% citric acid (500 mL), sat. NaHCO$_3$ (250 mL), and brine (200 mL), and dried over Na$_2$SO$_4$. Concentration of the solvent gave **10** (157 g) as a colorless viscous oil. ^{1}H NMR (400 MHz, DMSO-d_6): δ 7.83−7.75 (m, 3H), 6.94 (br s, 1H), 6.78−6.7 (m, 3H), 3.56 (s, 3H), 3.58−3.48 (m, 12H), 3.02 (q, J = 6.6 Hz, 6H), 2.9 (q, J = 6.4 Hz, 6H), 2.3−2.22 (m, 8H), 2.04 (t, J = 7.4 Hz, 2H), 1.55−1.4 (m, 10H), 1.36 (s, 27H), 1.22 (br s, 12H). ^{13}C NMR (101 MHz, CDCl$_3$): δ 174.0, 173.8, 171.5, 156.2, 78.5, 69.1, 67.1, 59.3, 51.1, 37.0, 36.7, 36.2, 35.9, 33.6, 29.6, 29.1, 29.0, 28.8, 28.7, 28.1, 24.5. HRMS calcd for C$_{50}$H$_{93}$N$_7$NaO$_{15}$ [M + Na]$^+$, 1054.6627; found, 1054.6626.

Compound 15. To a stirred solution of **10** (135 g, 131 mmol) in 1.5 L of THF was added aq. LiOH (13 g in 0.5 L of water, 309.5 mmol). The reaction was stirred at room temperature for 14 h. The solvent was evaporated to ~1, and 2 L of water were added. This aqueous solution was washed twice with 1 L ethyl acetate, and the pH was adjusted to 2−3 with 20% citric acid. After extraction with DCM (1 L twice), the product was washed with brine, dried over Na$_2$SO$_4$, and concentrated to yield **11** (107 g) as a colorless viscous oil. To a stirred solution of crude **11** (100 g, 98.42 mmol) in 250 mL of DMF was added 500 mL of 4 M HCl in dioxane, and the reaction was stirred overnight. Another 250 mL of 4 M HCl in dioxane was added, and the reaction was stirred for 6 h. Subsequently, 1 L of dioxane was added, and the reaction mixture was allowed to stand overnight. The solvent was removed by decantation to yield **12** as a viscous oil. This material was dissolved in 230 mL of DMF, Et$_3$N (68.2 mL, 492.1

mmol) and ethyl trifluoroacetate (58.54 mL, 492.1 mmol) were added, and the reaction was stirred overnight at room temperature. Volatiles were removed by evaporation under reduced pressure followed by extraction with DCM. The solution was washed with 5% citric acid, water, and brine. The solvent was dried over anhydrous Na_2SO_4 and concentrated to yield **13** (~100 g) as colorless foam. This acid was dissolved in DMF (350 mL), and *trans* hydroxyl prolinol **14** (43.4 g, 103.5 mmol), HBTU (39.2 g, 103.5 mmol), and HOBt (17.8 g, 132 mmol) were added. DIEA (30.3 g, 1235 mmol) was added dropwise at room temperature over 5 min. The reaction was stirred at room temperature overnight. After this, 1000 mL of water was added, and the mixture was allowed to stand for 30 min. The water was decanted, and this procedure was repeated with 500 mL of water. The viscous material thus obtained was dissolved in 1 L of DCM and washed with water and brine and dried over Na_2SO_4. Concentration of the solvent gave the crude material which was purified by column chromatography to obtain **15** (80 g, 60%) as yellowish foamy solid. ^{1}H NMR (400 MHz, DMSO-d_6): δ 9.36 (s, 3H), 7.86 (t, *J* = 5.6 Hz, 3H), 7.33−7.16 (m, 9H), 6.95 (s, 1H), 6.90−6.80 (m, 4H), 4.95 (d, *J* = 4.0, 0.8H, major), 4.87 (d, *J* = 4.0 Hz, 0.2H, minor), 4.42−4.23 (m, 1H), 4.17−4.06 (m, 1H), 3.72 (s, 6H), 3.62−3.40 (m, 13H), 3.19−3.13 (m, 6H), 3.07−2.95 (m, 8H), 2.27 (t, *J* = 6.3 Hz, 6H), 2.19 (t, *J* = 7.4 Hz, 2H), 2.08−1.96 (m, 3H), 1.93−1.80 (m, 2H), 1.63−1.56 (m, 6H), 1.53−1.32 (m, 4H), 1.20 (s, 12H). ^{13}C NMR (101 MHz, DMSO-d_6): δ 172.5, 171.1 (minor), 171.0, 170.3, 158.1, 158.0, 156.6, 156.3, 156.0, 155.7, 145.1, 144.8, 135.9, 135.8, 135.5 (minor), 135.4 (minor), 129.6, 129.55, 127.8, 127.7, 127.6, 127.56, 126.7 (minor), 126.5, 119.4, 117.1, 114.8, 113.2, 113.1, 113.06, 112.5, 85.8, 85.1, 68.6, 68.3, 67.5 (minor), 67.3, 63.3, 59.5, 55.6, 55.0, 55.0, 55.0, 54.9, 53.4, 37.1, 36.3, 36.1, 36.0, 35.9, 34.2, 29.0, 28.9, 28.8, 28.8, 28.7, 28.6, 28.4, 25.3, 24.5. ^{19}F NMR (376 MHz, DMSO): δ −81.38. HRMS calcd for $C_{66}H_{91}F_9N_8NaO_{15}$ [M + Na]$^+$, 1429.6358; found, 1429.7299.

Solid Support 2. Compound **15** (14.0 g, 9.95 mmol), succinic anhydride (2.0 g, 20 mmol), and DMAP (3.65 g, 29.85 mmol) were dissolved in DCM and stirred for 14 h. The reaction mixture was concentrated under reduced pressure, and the desired product was purified by a short silica gel column using 10% MeOH in DCM as an eluent. The solvent was removed under reduced pressure, and the residue was dried overnight under high vacuum. The product obtained was dissolved in acetonitrile (300 mL), and HBTU (4.74 g, 12.5 mmol), DIEA (1.62 g, 12.6 mmol), and LCAA CPG support (70 g, amine content: 99 μmol/g) were added. The suspension was gently shaken at room temperature on a wrist-action shaker for 24 h then filtered and washed with DCM, 10% MeOH in DCM, DCM, and ether. The solid support was dried under vacuum for 2 h. The unreacted amines on the support were capped by stirring with 25% acetic anhydride/pyridine containing 1% Et$_3$N at room temperature for 2 h. The support was washed with DCM, 10% MeOH in DCM, DCM, and ether then dried under vacuum for 2 h to yield solid support **2** (74.0 g, 58.0 μmol/g loading).

Synthesis of GalNAc-Conjugated siRNAs. Oligonucleotides (Supporting Information, Section II; Table 1) were synthesized on an ABI Synthesizer using commercially available 5′-*O*-(4,4′-dimethoxytrityl)-2′-deoxy-2′-fluoro-, 5′-*O*-(4,4′-dimethoxytrityl)-2′-*O*-(*tert*-butyldimethylsilyl)-, and 5′-*O*-(4,4′-dimethoxytrityl)-2′-*O*-methyl-3′-*O*-(2-cyanoethyl-*N*,*N*-diisopropyl) phosphoramidite monomers of uridine, 4-*N*-acetylcytidine, 6-*N*-benzoyladenosine, and 2-*N*-isobutyrylguanosine using standard solid-phase oligonucleotide synthesis and deprotection protocols.

The triantennary amine-functionalized sense strand **3** was synthesized from the solid support **2**, and antisense strands **40** and **42** (Table S1) were synthesized using standard solid-phase synthesis conditions. Two consecutive couplings of the phosphoramidite under solid-phase conditions to the solid support, followed by syntheses of the oligonucleotides[15] with desired chemistries, afforded the serial (1 + 1 + 1) triamine containing sense strands **39** or **41** (Table S1).

After completion of the automated synthesis, the solid support was washed with 0.1 M piperidine in acetonitrile for 10 min, then washed with anhydrous acetonitrile and dried with argon. The support was

then treated with 40% aqueous methylamine (1.5 mL/1 μmol of solid support) at 55 °C for 1 h to remove protecting groups from the oligonucleotides. The suspension was filtered through a 0.2 μm filter to remove solid residues, and the support was rinsed with deionized water. The oligonucleotides were purified by anion-exchange high-performance liquid chromatography (IEX-HPLC) with TSK-Gel Super Q-5PW support (TOSOH Corp.) using a linear gradient of 22−42% buffer B over 130 min with a 50 mL/min flow rate (buffer A: 0.02 M Na$_2$HPO$_4$ in 10% CH$_3$CN, pH 8.5, and buffer B: buffer A plus 1 M NaBr). All single strands were purified to >85% HPLC (260 nm) purity and then desalted by size exclusion chromatography on an AKTA Prime chromatography system using an AP-2 glass column (20 × 300 mm, Waters) custom-packed with Sephadex G25 (GE Healthcare), eluted with sterile nuclease-free water. The isolated yields for the oligonucleotides were calculated based on the respective ratios of measured to theoretical 260 nm optical density units. The integrities of the purified oligonucleotides were confirmed by LC−MS (Supporting Information, Section IV) and by analytical IEX HPLC.

Post-synthetic Conjugation of GalNAc and Anomeric Linkage-Modified GalNAc to Sense Strands. The triamine-functionalized sense strands **3**, **39**, and **41** (Scheme 2 and Supporting Information Section II, Table 1) were separately and chemoselectively coupled with GalNAc and anomeric-linkage modified GalNAc NHS esters **4** and **16**−**22** to obtain the corresponding triantennary and serial (1 + 1 + 1) GalNAc-containing sense strands **23**−**30** and **31**−**38**, respectively. In brief, the amine-modified oligonucleotide was dissolved at a concentration of approximately 20 mg/mL in a 0.05 M sodium phosphate buffer at pH 7.1. 10 equiv of the NHS ester was dissolved in ACN in the same volume as the phosphate buffer. The NHS ester solution was added to the aqueous oligonucleotide solution and shaken at room temperature. The progress of the reaction was monitored hourly by LC/MS. After completion of the reaction, at approximately 3 h, an equal volume of aqueous methylamine was added to deprotect the acetate on the sugar moieties. The mixture was shaken at room temperature for 4 h, yielding completely deprotected GalNAc-conjugated sense strands. The crude GalNAc-conjugated siRNAs were purified by IEX-HPLC and then desalted by size exclusion chromatography as described above. The integrity of each modified sense strand was confirmed by LC−MS analysis (Supporting Information Sections II and IV, Table S1). Equimolar amounts of complementary sense **23**−**38** and antisense **40** strands were mixed and annealed by heating in a water bath at 95 °C for 5 min and cooling to room temperature to obtain the desired siRNAs **I**−**XVI**. The siRNA samples were analyzed for purity, endotoxin, and osmolality,[14,15] and the observed values were within the allowed range for the concentration tested.

ASGPR Binding Studies. Freshly isolated hepatocytes were resuspended at 1 million cells per mL in Dulbecco's modified Eagle Medium (Life Technologies) with 2% bovine serum albumin (BSA, Sigma-Aldrich), and binding to ASGPR was evaluated using a previously described flow cytometry-based competitive binding assay.[22] The GalNAc$_3$-conjugated, Alexa647-labeled siRNA[54] was diluted to a final concentration of 20 nM and premixed with unlabeled siRNA **I**−**XVI** at an appropriate range of final concentrations from 3 μM to 1.4 nM in Dulbecco's Modified Eagle Medium with 2% BSA. To wells containing siRNA, 100,000 hepatocytes were added, and samples were incubated at 4 °C for 15 min. Cells were washed twice with Dulbecco's phosphate-buffered saline with Mg/Ca (Life Technologies) with 2% BSA. Samples were centrifuged at 50g for 3 min to pellet cells between washes. Cells were resuspended in a solution of Dulbecco's phosphate-buffered saline with Mg/Ca with 2% BSA and propidium iodide (Sigma-Aldrich) and analyzed on an LSRII flow cytometer (BD Biosciences). Compensation was performed using Diva software (BD Biosciences). Hepatocytes were gated by size using forward scatter and side scatter, and dead cells, identified based on propidium iodide staining, were excluded from analysis. The median fluorescence intensity of the Alexa647 siRNA was quantified. Data were analyzed using FlowJo and GraphPad Prism.

In Vitro Gene Silencing Experiments. *Transfection Experiments.* To the wells of a 384-well plate were added 2.5 μL of siRNA duplex **I-XVI**, 7.4 μL of Opti-MEM, and 0.1 μL of Lipofectamine RNAiMax (Invitrogen). Samples were incubated at room temperature for 15 min. Primary mouse hepatocytes ($\sim$5 × 10^3 cells in 40 μL of William's E Medium, Life Technology) were then added to the siRNA mixture. Cells were incubated for 24 h. RNA was purified, and levels of targeted mRNA were determined. Each sample was run in technical duplicate. Dose response experiments were done over a range of doses from 0.01 to 100 nM final duplex concentration. *GAPDH* was quantified as the internal control. Values are plotted as a fraction of untreated control cells, and each point represents the mean of two biological samples ± percent error. IC$_{50}$ values and dose–response curves were generated using XLFit software.

Free Uptake Experiments. To the wells of a 384-well plate were added 2.5 μL of siRNA duplex **I−XVI** and 40 μL of William's E Medium containing $\sim$5 × 10^3 primary mouse hepatocytes. Cells were incubated at 37 °C and 5% CO$_2$ for 24 h. RNA was purified, and levels of targeted mRNA were determined. Each sample was run in technical duplicate. Dose response experiments were done over a range of doses from 100 to 0.01 nM final duplex concentration. *GAPDH* was quantified as the internal control. Values are plotted as a fraction of untreated control cells, and each point represents the mean of two biological samples ± percent error. IC$_{50}$ values and dose–response curves were generated using XLFit software.

Analysis of Silencing Activity in Mice. All procedures involving mice were conducted by certified laboratory personnel using protocols consistent with local, state, and federal regulations. Experimental protocols were approved by the Institutional Animal Care and Use Committee (IACUC), the Association for Assessment and Accreditation of Laboratory Animal Care International (accreditation number: 001345), and the office of Laboratory Animal Welfare (accreditation number: A4517-01). When deciding on sample numbers for animal studies, we determined the final number required to ensure confidence in the resulting data while utilizing the least number of animals, as required by IACUC guidelines. Female C57/BL6 mice of approximately 8 weeks of age were obtained from Charles River Laboratories and randomly assigned to each group. Mice were acclimated in-house for 48 h prior to study start.

Animals were dosed subcutaneously at 10 μL/g with siRNA or with PBS saline control. Doses used in this study were 3, 1, or 0.3 mg/kg. The test compounds were diluted into PBS, pH 7.4. All solutions were stored at 4 °C until the time of injection. Animals were sacrificed at 4, 7, 13, 20, 27, or 34 days post-dose. Livers were harvested and snap-frozen for analysis. Blood was collected utilizing the retro-orbital eye bleed procedure 24 h after the final dose in accordance with the IACUC-approved protocol into Becton Dickinson serum separator tubes (Fisher Scientific, Cat# BD365967). For the metabolite study, animals were dosed at 10 mg/kg, and livers were harvested at 0.25, 2, or 8 h post-dose.

For analysis of TTR, serum samples were kept at room temperature for 1 h and then spun in a microcentrifuge at 21,000g at room temperature for 10 min. Serum was transferred into 1.5 mL microcentrifuge tubes for storage at −80 °C until the time of assay. Serum samples were diluted 1:4000 and assayed using a commercially available kit from ALPCO (Cat# 41-PALMS-E01). Protein concentrations (μg/mL) were determined by comparison to a purified TTR standard, and the manufacturer's instructions were followed.

Determination of Liver Levels of Antisense Strand. Aliquots of the tissue (frozen, powdered) were reconstituted to 100 mg/mL concentration in PBS with 0.25% Triton X-100 and lysed by boiling. The supernatant was used to generate antisense-specific cDNA using sequence-specific stem loop cDNA primer; a sequence-specific TaqMan assay, and the Light Cycler 480 system (Roche). siRNA concentrations were determined by extrapolation from the standard curves generated by spiking the naïve tissue with various concentrations of synthetic siRNAs.

■ ASSOCIATED CONTENT

Ⓢ Supporting Information

The Supporting Information is available free of charge at https://pubs.acs.org/doi/10.1021/acs.jmedchem.2c01337.

Structure of triantennary GalNAc−siRNAs with the standard β-*O*-glycosidic linkage; oligonucleotide characterization; ^{1}H, ^{13}C, and ^{31}P NMR spectra of selected compounds; and LC−MS profiles of selected GalNAc-conjugated strands (PDF)

Molecular formula strings (CSV)

■ AUTHOR INFORMATION

Corresponding Author

    Muthiah Manoharan − *Alnylam Pharmaceuticals, Inc., Cambridge, Massachusetts 02142, United States;* ⓞ orcid.org/0000-0002-7931-1172; Email: mmanoharan@alnylam.com

Authors

    Pachamuthu Kandasamy − *Alnylam Pharmaceuticals, Inc., Cambridge, Massachusetts 02142, United States*

    Shohei Mori − *Alnylam Pharmaceuticals, Inc., Cambridge, Massachusetts 02142, United States;* ⓞ orcid.org/0000-0001-8472-8055

    Shigeo Matsuda − *Alnylam Pharmaceuticals, Inc., Cambridge, Massachusetts 02142, United States*

    Namrata Erande − *Alnylam Pharmaceuticals, Inc., Cambridge, Massachusetts 02142, United States*

    Dhrubajyoti Datta − *Alnylam Pharmaceuticals, Inc., Cambridge, Massachusetts 02142, United States*

    Jennifer L. S. Willoughby − *Alnylam Pharmaceuticals, Inc., Cambridge, Massachusetts 02142, United States*

    Nate Taneja − *Alnylam Pharmaceuticals, Inc., Cambridge, Massachusetts 02142, United States*

    Jonathan O'Shea − *Alnylam Pharmaceuticals, Inc., Cambridge, Massachusetts 02142, United States*

    Anna Bisbe − *Alnylam Pharmaceuticals, Inc., Cambridge, Massachusetts 02142, United States*

    Rajar M. Manoharan − *Alnylam Pharmaceuticals, Inc., Cambridge, Massachusetts 02142, United States*

    Kristina Yucius − *Alnylam Pharmaceuticals, Inc., Cambridge, Massachusetts 02142, United States*

    Tuyen Nguyen − *Alnylam Pharmaceuticals, Inc., Cambridge, Massachusetts 02142, United States*

    Ramesh Indrakanti − *Alnylam Pharmaceuticals, Inc., Cambridge, Massachusetts 02142, United States*

    Swati Gupta − *Alnylam Pharmaceuticals, Inc., Cambridge, Massachusetts 02142, United States*

    Jason A. Gilbert − *Alnylam Pharmaceuticals, Inc., Cambridge, Massachusetts 02142, United States*

    Tim Racie − *Alnylam Pharmaceuticals, Inc., Cambridge, Massachusetts 02142, United States*

    Amy Chan − *Alnylam Pharmaceuticals, Inc., Cambridge, Massachusetts 02142, United States*

    Ju Liu − *Alnylam Pharmaceuticals, Inc., Cambridge, Massachusetts 02142, United States;* ⓞ orcid.org/0000-0003-1030-9266

    Renta Hutabarat − *Alnylam Pharmaceuticals, Inc., Cambridge, Massachusetts 02142, United States*

    Jayaprakash K. Nair − *Alnylam Pharmaceuticals, Inc., Cambridge, Massachusetts 02142, United States*

Klaus Charisse − *Alnylam Pharmaceuticals, Inc., Cambridge, Massachusetts 02142, United States*

Martin A. Maier − *Alnylam Pharmaceuticals, Inc., Cambridge, Massachusetts 02142, United States*

Kallanthottathil G. Rajeev − *Alnylam Pharmaceuticals, Inc., Cambridge, Massachusetts 02142, United States;* ⊙ orcid.org/0000-0002-0104-0237

Martin Egli − *Department of Biochemistry, School of Medicine, Vanderbilt University, Nashville, Tennessee 37232, United States;* ⊙ orcid.org/0000-0003-4145-356X

Complete contact information is available at:
https://pubs.acs.org/10.1021/acs.jmedchem.2c01337

Notes

The authors declare no competing financial interest.

■ ABBREVIATIONS

ASGPR, asialoglycoprotein receptor; brs, broad signal; BSA, bovine serum albumin; CRD, carbohydrate recognition domain; d, doublet; ED_{50}, median effective dose; IACUC, Institutional Animal Care and Use Committee; IC_{50}, half-maximal inhibitory concentrations; K_i, inhibitory constants; m, multiplet; GalNAc, *N*-acetyl-D-galactosamine; RNAi, RNA interference; s, singlet; siRNA, small interfering RNA; t, triplet

■ REFERENCES

(1) Balwani, M.; Sardh, E.; Ventura, P.; Peiró, P. A.; Rees, D. C.; Stölzel, U.; Bissell, D. M.; Bonkovsky, H. L.; Windyga, J.; Anderson, K. E.; Parker, C.; Silver, S. M.; Keel, S. B.; Wang, J.-D.; Stein, P. E.; Harper, P.; Vassiliou, D.; Wang, B.; Phillips, J.; Ivanova, A.; Langendonk, J. G.; Kauppinen, R.; Minder, E.; Horie, Y.; Penz, C.; Chen, J.; Liu, S.; Ko, J. J.; Sweetser, M. T.; Garg, P.; Vaishnaw, A.; Kim, J. B.; Simon, A. R.; Gouya, L. Phase 3 Trial of RNAi Therapeutic Givosiran for Acute Intermittent Porphyria. *N. Engl. J. Med.* **2020**, *382*, 2289−2301.

(2) Liebow, A.; Li, X.; Racie, T.; Hettinger, J.; Bettencourt, B. R.; Najafian, N.; Haslett, P.; Fitzgerald, K.; Holmes, R. P.; Erbe, D.; Querbes, W.; Knight, J. An Investigational RNAi Therapeutic Targeting Glycolate Oxidase Reduces Oxalate Production in Models of Primary Hyperoxaluria. *J. Am. Soc. Nephrol.* **2017**, *28*, 494−503.

(3) Fitzgerald, K.; White, S.; Borodovsky, A.; Bettencourt, B. R.; Strahs, A.; Clausen, V.; Wijngaard, P.; Horton, J. D.; Taubel, J.; Brooks, A.; Fernando, C.; Kauffman, R. S.; Kallend, D.; Vaishnaw, A.; Simon, A. A Highly Durable RNAi Therapeutic Inhibitor of PCSK9. *N. Engl. J. Med.* **2017**, *376*, 41−51.

(4) Raal, F. J.; Kallend, D.; Ray, K. K.; Turner, T.; Koenig, W.; Wright, R. S.; Wijngaard, P. L. J.; Curcio, D.; Jaros, M. J.; Leiter, L. A.; Kastelein, J. J. P. Inclisiran for the Treatment of Heterozygous Familial Hypercholesterolemia. *N. Engl. J. Med.* **2020**, *382*, 1520−1530.

(5) Ray, K. K.; Wright, R. S.; Kallend, D.; Koenig, W.; Leiter, L. A.; Raal, F. J.; Bisch, J. A.; Richardson, T.; Jaros, M.; Wijngaard, P. L. J.; Kastelein, J. J. P. Two Phase 3 Trials of Inclisiran in Patients with Elevated LDL Cholesterol. *N. Engl. J. Med.* **2020**, *382*, 1507−1519.

(6) Gonzalez-Duarte, A.; Adams, D.; Tournev, I.; Taylor, M.; Coelho, T.; Plante-Bordeneuve, V.; Berk, J.; Gillmore, J. D.; Low, S.-C.; Sekijima, Y.; Obici, L.; Chen, C.; Badri, P.; Arum, S.; Vest, J.; Polydefkis, M. Helios-a: results from the phase 3 study of vutrisiran in

patients with hereditary transthyretin-mediated amyloidosis with polyneuropathy. *J. Am. Coll. Cardiol.* **2022**, *79*, 302.

(7) Onizuka, T.; Shimizu, H.; Moriwaki, Y.; Nakano, T.; Kanai, S.; Shimada, I.; Takahashi, H. NMR study of ligand release from asialoglycoprotein receptor under solution conditions in early endosomes. *FEBS J.* **2012**, *279*, 2645−2656.

(8) Grewal, P. K. The Ashwell−Morell Receptor. In *Methods in Enzymology*; Fukuda, M., Ed.; Academic Press, 2010; Chapter 13, Vol. *479*, pp 223−241.

(9) Schwartz, A. L.; Rup, D.; Lodish, H. F. Difficulties in the quantification of asialoglycoprotein receptors on the rat hepatocyte. *J. Biol. Chem.* **1980**, *255*, 9033−9036.

(10) Spiess, M. The asialoglycoprotein receptor: a model for endocytic transport receptors. *Biochemistry* **1990**, *29*, 10009−10018.

(11) Steirer, L. M.; Park, E. I.; Townsend, R. R.; Baenziger, J. U. The asialoglycoprotein receptor regulates levels of plasma glycoproteins terminating with sialic acid alpha2,6-galactose. *J. Biol. Chem.* **2009**, *284*, 3777−3783.

(12) Nair, J. K.; Willoughby, J. L. S.; Chan, A.; Charisse, K.; Alam, M. R.; Wang, Q.; Hoekstra, M.; Kandasamy, P.; Kel'in, A. V.; Milstein, S.; Taneja, N.; O'Shea, J.; Shaikh, S.; Zhang, L.; van der Sluis, R. J.; Jung, M. E.; Akinc, A.; Hutabarat, R.; Kuchimanchi, S.; Fitzgerald, K.; Zimmermann, T.; van Berkel, T. J. C.; Maier, M. A.; Rajeev, K. G.; Manoharan, M. Multivalent N-Acetylgalactosamine-Conjugated siRNA Localizes in Hepatocytes and Elicits Robust RNAi-Mediated Gene Silencing. *J. Am. Chem. Soc.* **2014**, *136*, 16958−16961.

(13) Manoharan, M.; Rajeev, K. G.; Narayanannair, J. K.; Maier, M. Preparation of oligosaccharide-DNA duplexes as delivery agents for oligonucleotides. WO 2009073809 A2, 2009.

(14) Matsuda, S.; Keiser, K.; Nair, J. K.; Charisse, K.; Manoharan, R. M.; Kretschmer, P.; Peng, C. G.; V. Kel'in, V.; Willoughby, P.; Liebow, J. L. S.; Querbes, A.; Yucius, W.; Nguyen, K.; Milstein, T.; Maier, S.; Rajeev, M. A.; Manoharan, K. G.; Manoharan, M. siRNA Conjugates Carrying Sequentially Assembled Trivalent N-Acetylga-lactosamine Linked Through Nucleosides Elicit Robust Gene Silencing In Vivo in Hepatocytes. *ACS Chem. Biol.* **2015**, *10*, 1181−1187.

(15) Rajeev, K. G.; Nair, J. K.; Jayaraman, M.; Charisse, K.; Taneja, N.; O'Shea, J.; Willoughby, J. L. S.; Yucius, K.; Nguyen, T.; Shulga-Morskaya, S.; Milstein, S.; Liebow, A.; Querbes, W.; Borodovsky, A.; Fitzgerald, K.; Maier, M. A.; Manoharan, M. Hepatocyte-Specific Delivery of siRNAs Conjugated to Novel Non-nucleosidic Trivalent N-Acetylgalactosamine Elicits Robust Gene Silencing in Vivo. *ChemBioChem* **2015**, *16*, 903−908.

(16) Yamamoto, T.; Sawamura, M.; Wada, F.; Harada-Shiba, M.; Obika, S. Serial incorporation of a monovalent GalNAc phosphor-amidite unit into hepatocyte-targeting antisense oligonucleotides. *Bioorg. Med. Chem.* **2016**, *24*, 26−32.

(17) Sharma, V. K.; Osborn, M. F.; Hassler, M. R.; Echeverria, D.; Ly, S.; Ulashchik, E. A.; Martynenko-Makaev, Y. V.; Shmanai, V. V.; Zatsepin, T. S.; Khvorova, A.; Watts, J. K. Novel Cluster and Monomer-Based GalNAc Structures Induce Effective Uptake of siRNAs in Vitro and in Vivo. *Bioconjugate Chem.* **2018**, *29*, 2478−2488.

(18) Baenziger, J. U.; Maynard, Y. Human hepatic lectin. Physiochemical properties and specificity. *J. Biol. Chem.* **1980**, *255*, 4607−4613.

(19) Baenziger, J. U.; Fiete, D. Galactose and N-acetylgalactosamine-specific endocytosis of glycopeptides by isolated rat hepatocytes. *Cell* **1980**, *22*, 611−620.

(20) Kolatkar, A. R.; Weis, W. I. Structural Basis of Galactose Recognition by C-type Animal Lectins. *J. Biol. Chem.* **1996**, *271*, 6679−6685.

(21) Kolatkar, A. R.; Leung, A. K.; Isecke, R.; Brossmer, R.; Drickamer, K.; Weis, W. I. Mechanism of N-Acetylgalactosamine Binding to a C-type Animal Lectin Carbohydrate-recognition Domain. *J. Biol. Chem.* **1998**, *273*, 19502−19508.

(22) Meier, M.; Bider, M. D.; Malashkevich, V. N.; Spiess, M.; Burkhard, P. Crystal structure of the carbohydrate recognition domain

of the H1 subunit of the asialoglycoprotein receptor. *J. Mol. Biol.* **2000**, *300*, 857−865.

(23) Wong, T. C.; Townsend, R. R.; Lee, Y. C. Synthesis of D-galactosamine derivatives and binding studies using isolated rat hepatocytes. *Carbohydr. Res.* **1987**, *170*, 27−46.

(24) Khorev, O.; Stokmaier, D.; Schwardt, O.; Cutting, B.; Ernst, B. Trivalent, Gal/GalNAc-containing ligands designed for the asialoglycoprotein receptor. *Bioorg. Med. Chem.* **2008**, *16*, 5216−5231.

(25) Stokmaier, D.; Khorev, O.; Cutting, B.; Born, R.; Ricklin, D.; Ernst, T. O. G.; Böni, F.; Schwingruber, K.; Gentner, M.; Wittwer, M.; Spreafico, M.; Vedani, A.; Rabbani, S.; Schwardt, O.; Ernst, B. Design, synthesis and evaluation of monovalent ligands for the asialoglycoprotein receptor (ASGP-R). *Bioorg. Med. Chem.* **2009**, *17*, 7254−7264.

(26) Mamidyala, S. K.; Dutta, S.; Chrunyk, B. A.; Préville, C.; Wang, H.; Withka, J. M.; McColl, A.; Subashi, T. A.; Hawrylik, S. J.; Griffor, M. C.; Kim, S.; Pfefferkorn, J. A.; Price, D. A.; Menhaji-Klotz, E.; Mascitti, V.; Finn, M. G. Glycomimetic Ligands for the Human Asialoglycoprotein Receptor. *J. Am. Chem. Soc.* **2012**, *134*, 1978−1981.

(27) Sanhueza, C. A.; Baksh, M. M.; Thuma, B.; Roy, M. D.; Dutta, S.; Préville, C.; Chrunyk, B. A.; Beaumont, K.; Dullea, R.; Ammirati, M.; Liu, S.; Gebhard, D.; Finley, J. E.; Salatto, C. T.; King-Ahmad, A.; Stock, I.; Atkinson, K.; Reidich, B.; Lin, W.; Kumar, R.; Tu, M.; Menhaji-Klotz, E.; Price, D. A.; Liras, S.; Finn, M. G.; Mascitti, V. Efficient Liver Targeting by Polyvalent Display of a Compact Ligand for the Asialoglycoprotein Receptor. *J. Am. Chem. Soc.* **2017**, *139*, 3528−3536.

(28) Lee, S. S.; Yu, S.; Withers, S. G. Detailed Dissection of a New Mechanism for Glycoside Cleavage: α-1,4-Glucan Lyase. *Biochemistry* **2003**, *42*, 13081−13090.

(29) Yip, V. L. Y.; Withers, S. G. Nature's many mechanisms for the degradation of oligosaccharides. *Org. Biomol. Chem.* **2004**, *2*, 2707−2713.

(30) Lee, S. S.; Yu, S.; Withers, S. G. α-1,4-Glucan Lyase Performs a Trans-Elimination via a Nucleophilic Displacement Followed by a Syn-Elimination. *J. Am. Chem. Soc.* **2002**, *124*, 4948−4949.

(31) Prakash, T. P.; Graham, M. J.; Yu, J.; Carty, R.; Low, A.; Chappell, A.; Schmidt, K.; Zhao, C.; Aghajan, M.; Murray, H. F.; Riney, S.; Booten, S. L.; Murray, S. F.; Gaus, H.; Crosby, J.; Lima, W. F.; Guo, S.; Monia, B. P.; Swayze, E. E.; Seth, P. P. Targeted delivery of antisense oligonucleotides to hepatocytes using triantennary N-acetyl galactosamine improves potency 10-fold in mice. *Nucleic Acids Res.* **2014**, *42*, 8796−8807.

(32) Basiri, B.; Xie, F.; Wu, B.; Humphreys, S. C.; Lade, J. M.; Thayer, M. B.; Yamaguchi, P.; Florio, M.; Rock, B. M. Introducing an In Vitro Liver Stability Assay Capable of Predicting the In Vivo Pharmacodynamic Efficacy of siRNAs for IVIVC. *Mol. Ther. Nucleic Acids* **2020**, *21*, 725−736.

(33) Pachamuthu, K.; Schmidt, R. R. Synthetic Routes to Thiooligosaccharides and Thioglycopeptides. *Chem. Rev.* **2006**, *106*, 160−187.

(34) Ogata, M.; Hidari, K. I. P. J.; Kozaki, W.; Murata, T.; Hiratake, J.; Park, E. Y.; Suzuki, T.; Usui, T. Molecular Design of Spacer-N-Linked Sialoglycopolypeptide as Polymeric Inhibitors Against Influenza Virus Infection. *Biomacromolecules* **2009**, *10*, 1894−1903.

(35) McKay, M. J.; Nguyen, H. M. Recent developments in glycosyl urea synthesis. *Carbohydr. Res.* **2014**, *385*, 18−44.

(36) Dondoni, A.; Zuurmond, H. M.; Boscarato, A. Synthesis of α- and β-d-(1→6)-C-Disaccharides by Wittig Olefination of Formyl C-Glycosides with Glycopyranose 6-Phosphoranes. *J. Org. Chem.* **1997**, *62*, 8114−8124.

(37) Reddy, B. G.; Vankar, Y. D. The Synthesis of Hybrids of D-Galactose with 1-Deoxynojirimycin Analogues as Glycosidase Inhibitors. *Angew. Chem., Int. Ed.* **2005**, *44*, 2001−2004.

(38) Jacquinet, J.-C.; Zurabyan, S. E.; Khorlin, A. Y. Oxazoline synthesis of 1,2-trans-2-acetamido-2-deoxyglycosides. Glycosylation with 2-methyl-(3,4,6-tri-O-acetyl-1,2-dideoxy-α-D-galactopyrano)-[2′,1′:4,5]-2-oxazoline. *Carbohydr. Res.* **1974**, *32*, 137−143.

(39) Knapp, S.; Myers, D. S. Synthesis of α-GalNAc Thioconjugates from an α-GalNAc Mercaptan. *J. Org. Chem.* **2002**, *67*, 2995−2999.

(40) Sakamuri, S.; Eltepu, L.; Liu, D.; Lam, S.; Meade, B. R.; Liu, B.; Dello Iacono, G.; Kabakibi, A.; Luukkonen, L.; Leedom, T.; Foster, M.; Bradshaw, C. W. Impact of Phosphorothioate Chirality on Double-Stranded siRNAs: A Systematic Evaluation of Stereopure siRNA Designs. *ChemBioChem* **2020**, *21*, 1304−1308.

(41) Hsu, C.-H.; Park, S.; Mortenson, D. E.; Foley, B. L.; Wang, X.; Woods, R. J.; Case, D. A.; Powers, E. T.; Wong, C.-H.; Dyson, H. J.; Kelly, J. W. The Dependence of Carbohydrate−Aromatic Interaction Strengths on the Structure of the Carbohydrate. *J. Am. Chem. Soc.* **2016**, *138*, 7636−7648.

(42) Harrison, A. W.; Fisher, J. F.; Guido, D. M.; Couch, S. J.; Lawson, J. A.; Sutter, D. M.; Williams, M. V.; DeGraaf, G. L.; Rogers, J. E.; Pals, D. T.; DuCharme, D. W. Appraisal of a glycopeptide cloaking strategy for a therapeutic oligopeptide: Glycopeptide analogs of the renin inhibitor ditekiren. *Bioorg. Med. Chem.* **1994**, *2*, 1339−1361.

(43) Tanaka, M.; Yamashina, I. The syntheses of various 1-N-(L-aspart-4-oyl)-glycosylamines and their analogs. *Carbohydr. Res.* **1973**, *27*, 175−183.

(44) Dunstan, D.; Hough, L. The synthesis of 2-acetamido-1-N-(4-L-aspartyl)-2-deoxy-β-D-galactopyranosylamine. *Carbohydr. Res.* **1972**, *25*, 246−248.

(45) Brown, C. R.; Gupta, S.; Qin, J.; Racie, T.; He, G.; Lentini, S.; Malone, R.; Yu, M.; Matsuda, S.; Shulga-Morskaya, S.; Nair, A. V.; Theile, C. S.; Schmidt, K.; Shahraz, A.; Goel, V.; Parmar, R. G.; Zlatev, I.; Schlegel, M. K.; Nair, J. K.; Jayaraman, M.; Manoharan, M.; Brown, D.; Maier, M. A.; Jadhav, V. Investigating the pharmacodynamic durability of GalNAc−siRNA conjugates. *Nucleic Acids Res.* **2020**, *48*, 11827−11844.

(46) Manoharan, M.; Nair, J. K.; Kandasamy, P.; Matsuda, S.; Kelin, A. V.; Jayaraman, M.; Rajeev, K. G. Process for the preparation of oligonucleotide-ligand conjugates as drug delivery and immunostimulant agents. WO 2015006740 A2, 2015.

(47) Huang, Y. Preclinical and Clinical Advances of GalNAc-Decorated Nucleic Acid Therapeutics. *Mol. Ther. Nucleic Acids* **2017**, *6*, 116−132.

(48) Weingärtner, A.; Bethge, L.; Weiss, L.; Sternberger, M.; Lindholm, M. W. Less Is More: Novel Hepatocyte-Targeted siRNA Conjugates for Treatment of Liver-Related Disorders. *Mol. Ther. Nucleic Acids* **2020**, *21*, 242−250.

(49) Cui, H.; Zhu, X.; Li, S.; Wang, P.; Fang, J. Liver-Targeted Delivery of Oligonucleotides with N-Acetylgalactosamine Conjugation. *ACS Omega* **2021**, *6*, 16259−16265.

(50) Chong, S.; Agarwal, S.; Aluri, K. C.; Arciprete, M.; Brown, C.; Charisse, K.; Cichocki, J.; Fitzgerald, K.; Goel, V.; Gu, Y.; Guenther, D.; Habtemariam, B.; Jadhav, V.; Janas, M.; Jayaraman, M.; Kurz, J.; Li, J.; Liou, S.; Liu, J.; Liu, X.; Maclauchlin, C.; Maier, M.; Manoharan, M.; McDougall, R.; Nair, J.; Ramsden, D.; Robbie, G.; Schmidt, K.; Smith, P.; Theile, C.; Vaishnaw, A.; Waldron, S.; Wu, J.-T.; Xu, Y.; Zhang, X.; Zlatev, I.; castellanos-Rizaldos, E. The Nonclinical Disposition and PK/PD Properties of GalNAc-conjugated siRNA Are Highly Predictable and Build Confidence in Translation to Man. *Drug Metab. Dispos.* **2022**, *50*, 781−797.

(51) Holland, R. J.; Lam, K.; Ye, X.; Martin, A. D.; Wood, M. C.; Palmer, L.; Fraser, D.; McClintock, K.; Majeski, S.; Jarosz, A.; Lee, A. C. H.; Thi, E. P.; Judge, A.; Heyes, J. Ligand conjugate SAR and enhanced delivery in NHP. *Mol. Ther.* **2021**, *29*, 2910−2919.

(52) Ye, X.; Holland, R.; Wood, M.; Pasetka, C.; Palmer, L.; Samaridou, E.; McClintock, K.; Borisevich, V.; Geisbert, T. W.; Cross, R. W.; Heyes, J. Combination treatment of mannose and GalNAc conjugated small interfering RNA protects against lethal Marburg virus infection. *Mol. Ther.* **2023**, *31*, 269−281.

(53) Datta, D.; Mori, S.; Madaoui, M.; Wassarman, K.; Zlatev, I.; Manoharan, M. Aminooxy Click Chemistry as a Tool for Bis-homo and Bis-hetero Ligand Conjugation to Nucleic Acids. *Org. Lett.* **2022**, *24*, 4496−4501.

(54) Pettersen, E. F.; Goddard, T. D.; Huang, C. C.; Couch, G. S.; Greenblatt, D. M.; Meng, E. C.; Ferrin, T. E. UCSF Chimera—A visualization system for exploratory research and analysis. *J. Comput. Chem.* **2004**, *25*, 1605−1612.

📖 Recommended by ACS

Hiding Payload Inside the IgG Fc Cavity Significantly Enhances the Therapeutic Index of Antibody–Drug Conjugates

Wei Shi, Feng Tang, *et al.*

DECEMBER 30, 2022
JOURNAL OF MEDICINAL CHEMISTRY

READ 🗗

Degrader–Antibody Conjugates: Emerging New Modality

Ki Bum Hong and Hongchan An

DECEMBER 29, 2022
JOURNAL OF MEDICINAL CHEMISTRY

READ 🗗

Designing Synthetic, Sulfated Glycosaminoglycan Mimetics That Are Orally Bioavailable and Exhibiting *In Vivo* Anticancer Activity

Shravan Morla, Umesh R. Desai, *et al.*

JANUARY 12, 2023
JOURNAL OF MEDICINAL CHEMISTRY

READ 🗗

Self-Adjuvanting Protein Vaccine Conjugated with a Novel Synthetic TLR4 Agonist on Virus-Like Liposome Induces Potent Immunity against SARS-CoV-2

Dong Ding, Jun Guo, *et al.*

JANUARY 10, 2023
JOURNAL OF MEDICINAL CHEMISTRY

READ 🗗

Get More Suggestions >